Supporting Information

Dinuclear Group IV Metal Complexes based on a Bis(indenyl)-(*E*/*Z*)-Stilbene Platform: A Potential Prototype of "Photoswitchable" Catalysts for Olefin Polymerization

Nuria Romero,[1,a] Thierry Chavagnan,[1,a] Thierry Roisnel,[2] Alexandre Welle,[3]
Evgueni Kirillov,[1,*] and Jean-François Carpentier[1,*]

Table of contents

Figure S45. Representative DSC traces of ethylene / 1-hexene copolymer samples corresponding to a) NR2074, b) NR2077, c) NR2087, d) NR2149, e) NR2150, f) NR2141, g) NR2142, h) NR2132 and i) entries from Table S4.

Figure S46. Representative Size Exclusion Chromatography traces of polyethylene and ethylene / 1-hexe copolymer samples. a) Entry NR2108 from Table S2, b) Entry NR2130 from Table S2, c) Entry NR2132 from Table S4, d) Entry NR2133 from Table S4, e) Entry NR2137 from Table S2, f) Entry NR2141 from Table S4, g) Entry NR2142 from Table S4, h) Entry NR2146 from Table S2, i) Entry NR2149 from Table S4, j) Entry NR2150 from Table S4.

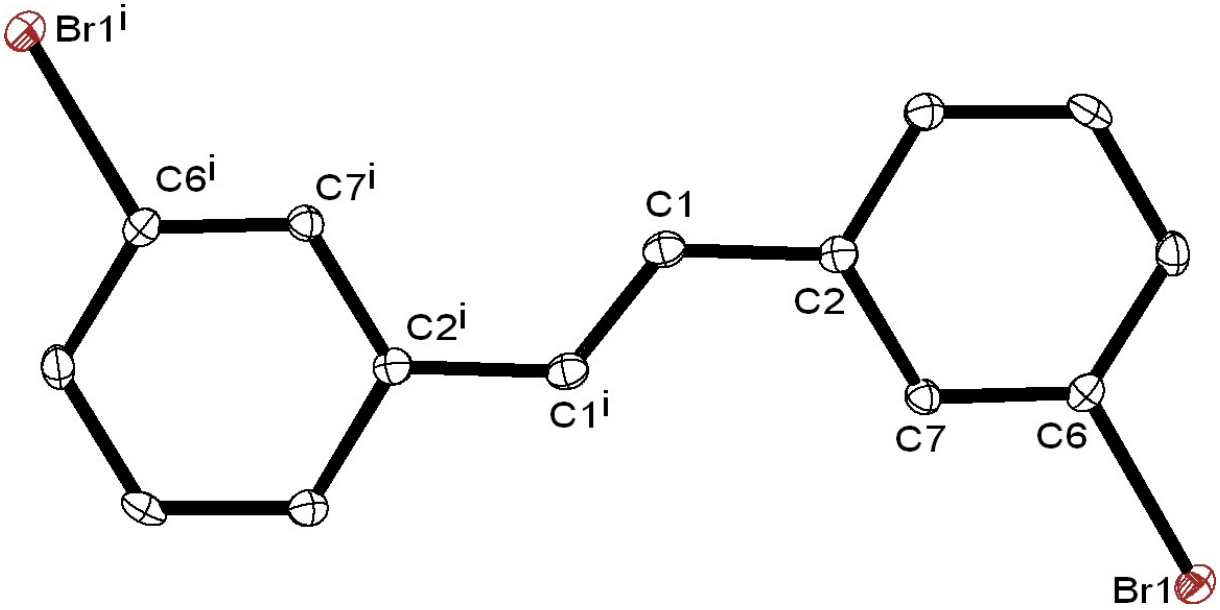

Figure S1. ORTEP plot of the solid-state molecular structure of (*E*)-3,3'-dibromostilbene (ellipsoids set at 50% probability level; all H atoms omitted for clarity). Selected bond distances (Å) and angles (°): C1–C1', 1.319(8); C6–Br1, 1.902(4); C2–C1, 1.468(5); C2–C1–C1'–C2, 180.0.

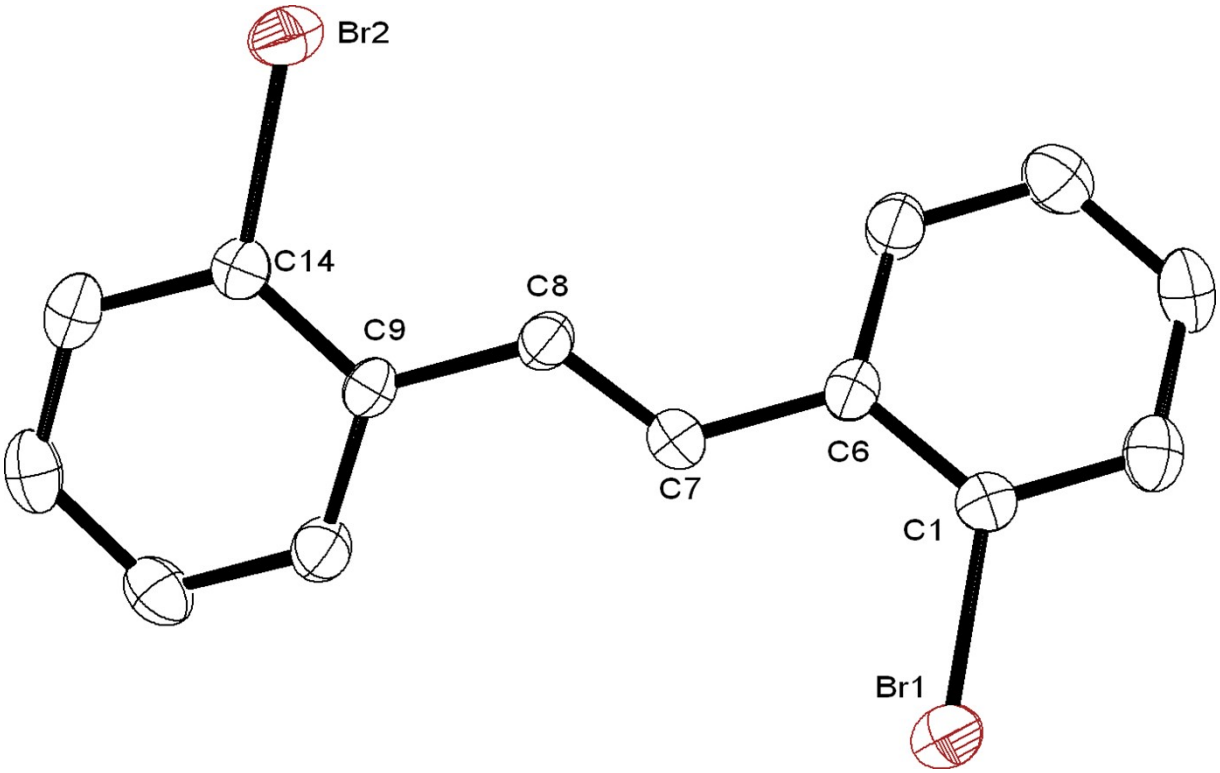

Figure S2. ORTEP plot of the solid-state molecular structure of (*E*)-2,2'-dibromostilbene (ellipsoids set at 50% probability level; all H atoms omitted for clarity). Selected bond distances (Å) and angles (°): C7–C8, 1.303(5); C1–Br1, 1.892(4); C6–C7, 1.460(5); C6–C7–C8–C9, 175.0(4).

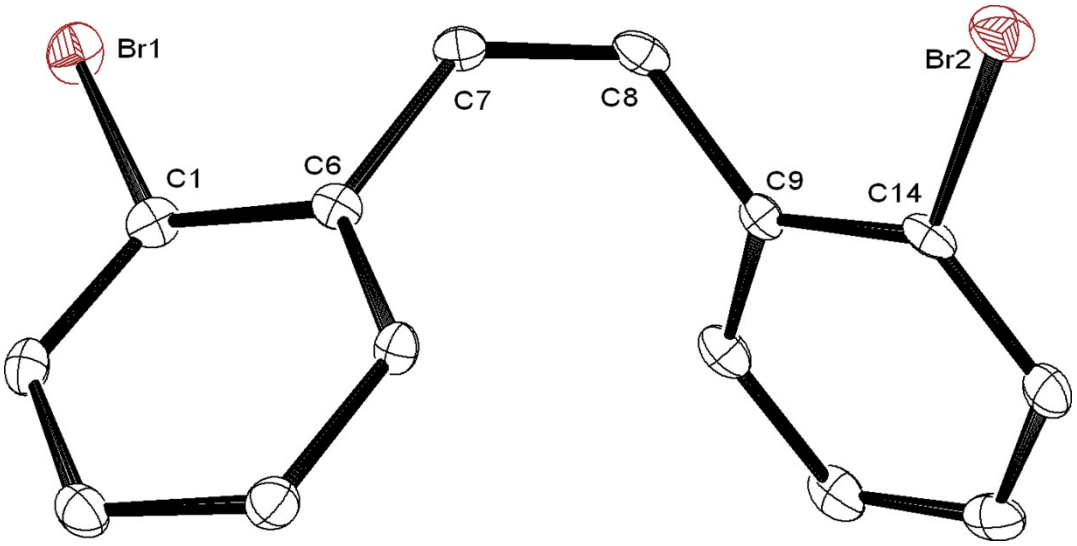

Figure S3. ORTEP plot of the solid-state molecular structure of (*Z*)-2,2'-dibromostilbene (ellipsoids set at 50% probability level; all H atoms omitted for clarity) (only one of the two independent molecules is depicted). Selected bond distances (Å) and angles (°): C7–C8, 1.333(4); C1–Br1, 1.912(3); C6–C7, 1.473(4); C6–C7–C8–C9, –8.0(5).

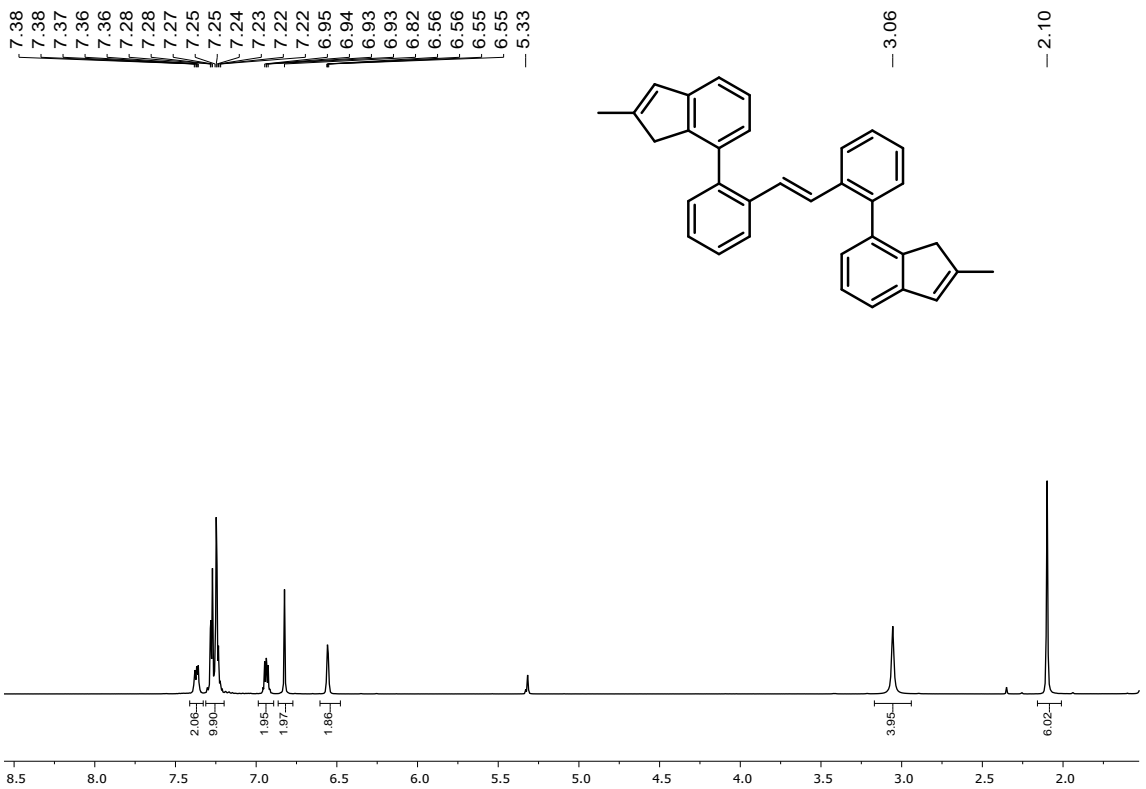

Figure S4. ^{1}H NMR spectrum (400 MHz, CD_2Cl_2, 23 °C) of {*o*-(*E*)-BisIndSB}H_2.

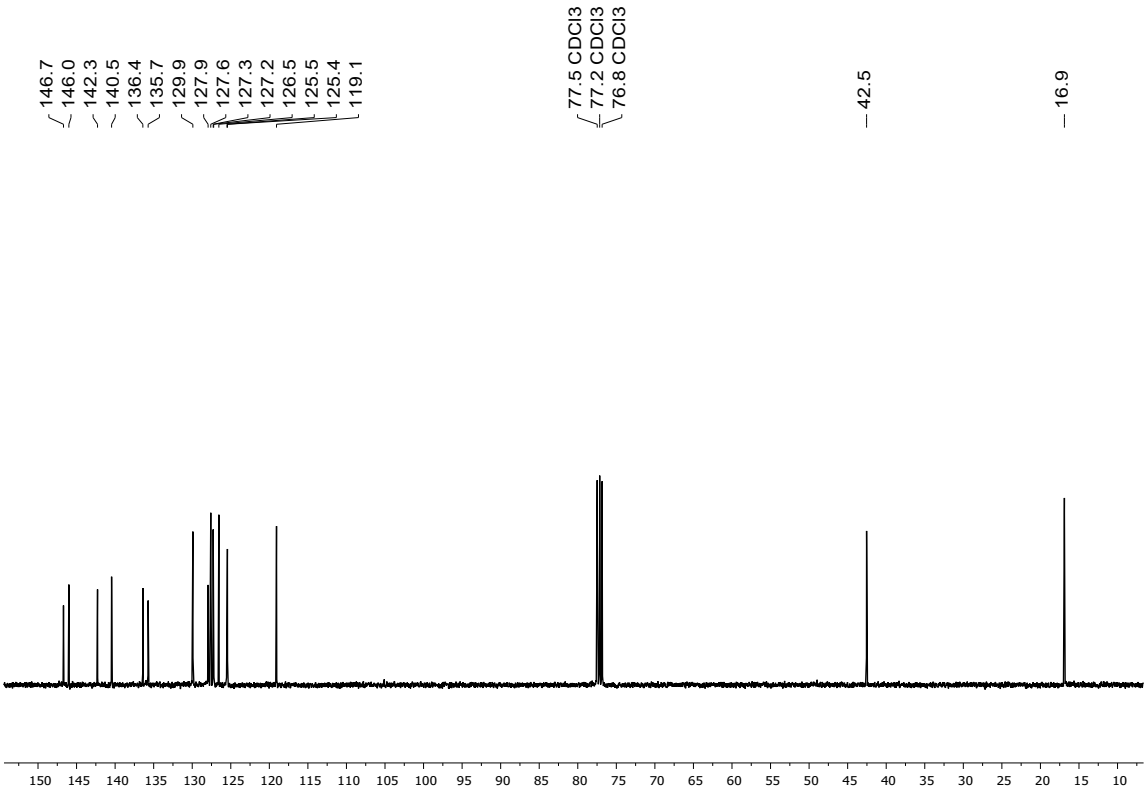

Figure S5. $^{13}C\{^{1}H\}$ NMR spectrum (101 MHz, CD_2Cl_2, 23 °C) of {*o*-(*E*)-BisIndSB}H_2.

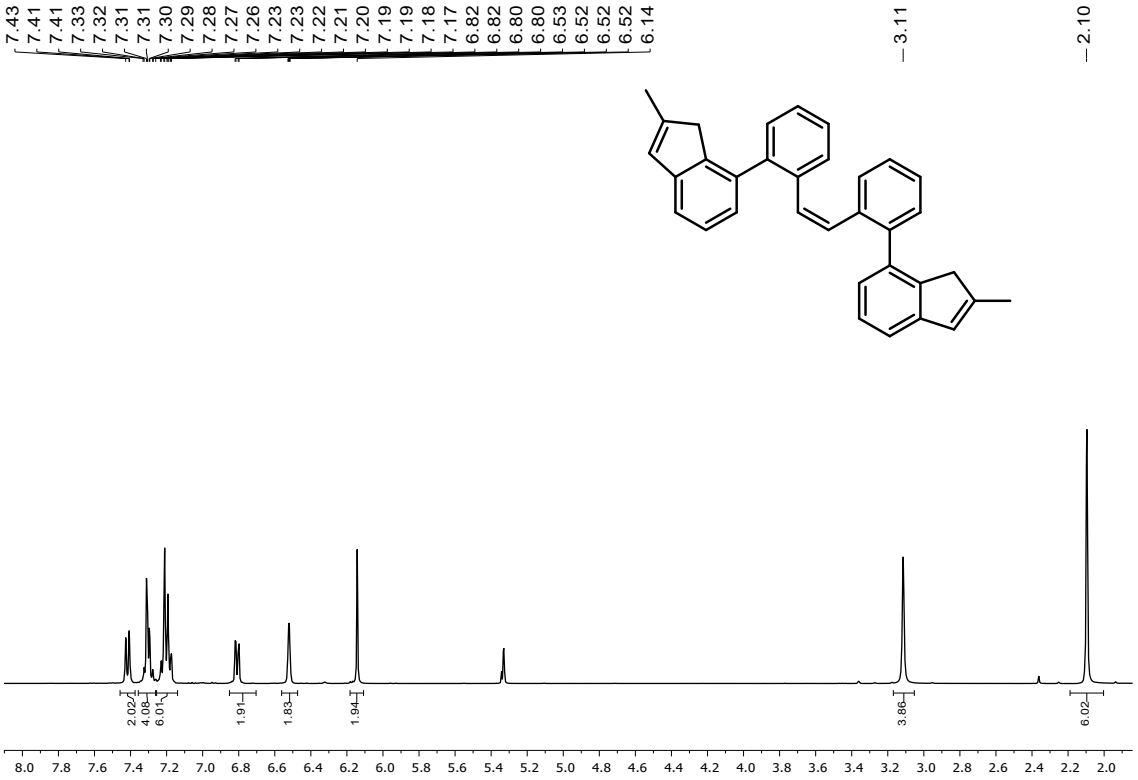

Figure S6. ^{1}H NMR spectrum (400 MHz, CD_2Cl_2, 23 °C) of {*o*-(*Z*)-BisIndSB}H_2.

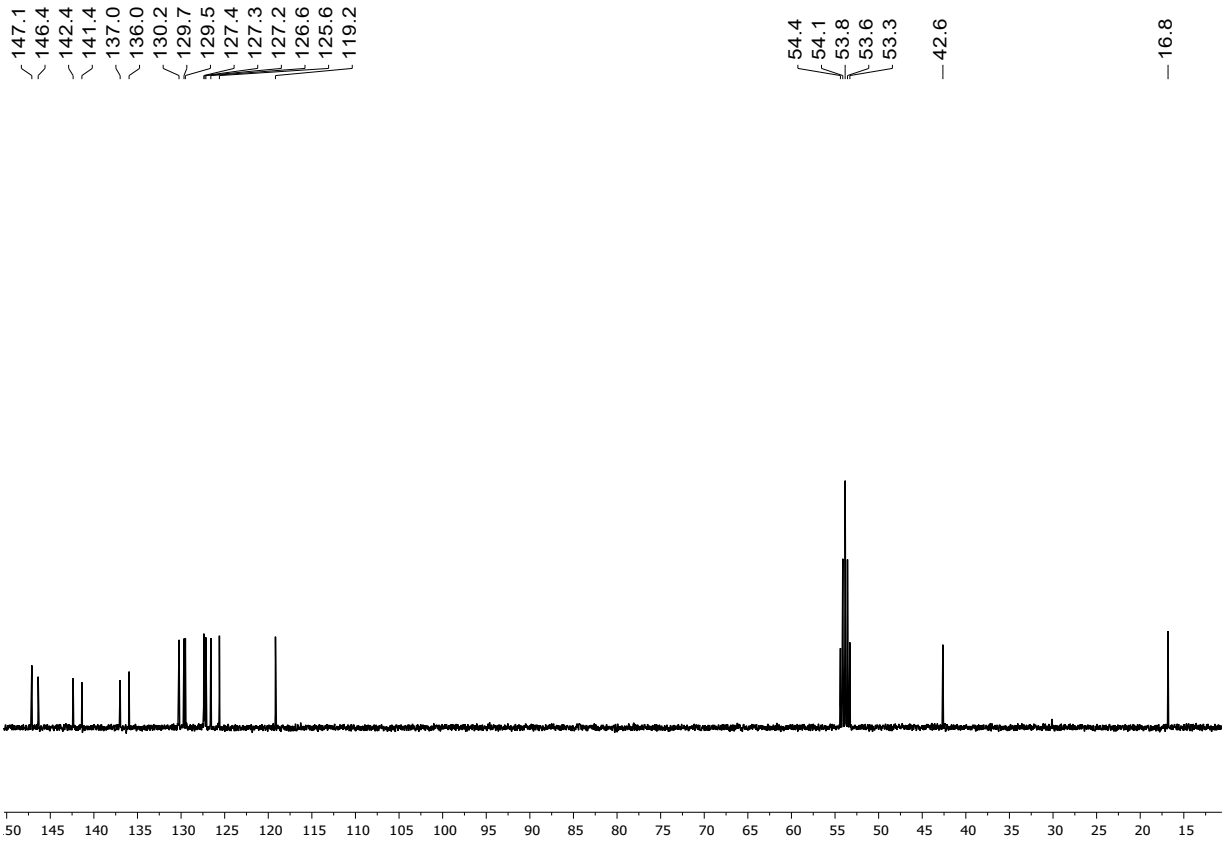

Figure S7. $^{13}C\{^{1}H\}$ NMR spectrum (101 MHz, CD_2Cl_2, 23 °C) of {*o*-(*Z*)-BisIndSB}H_2.

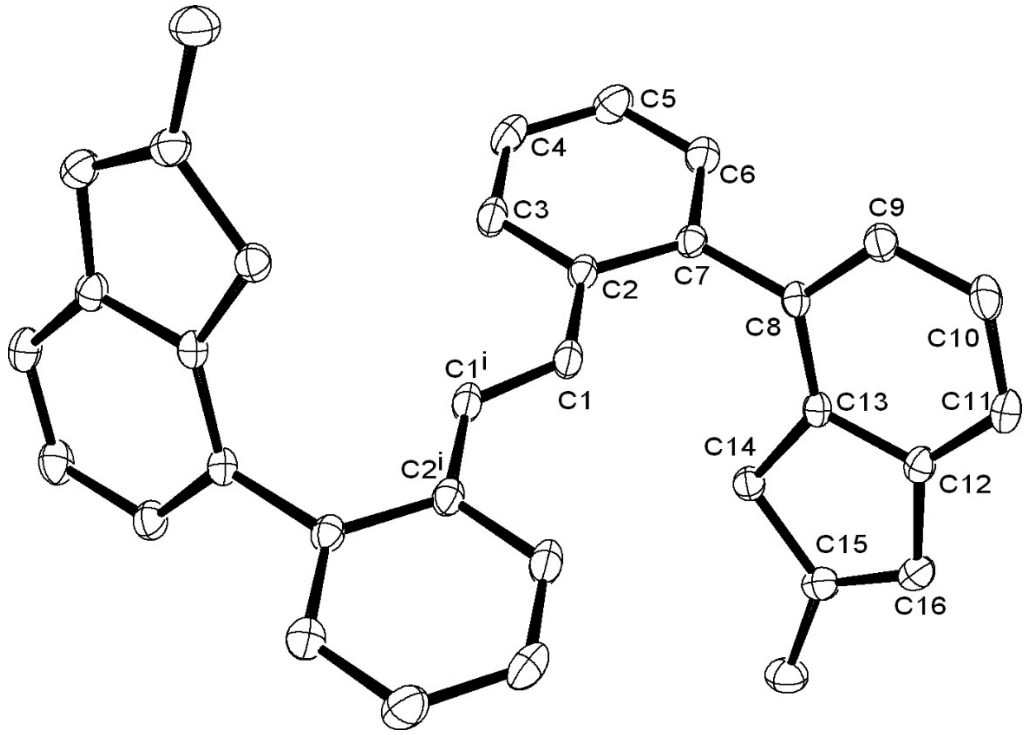

Figure S8. ORTEP plot of the solid-state molecular structure of {*o*-(*E*)-BisIndSB}H_2 (ellipsoids set at 50% probability level; all H atoms omitted for clarity). Selected bond distances (Å) and angles (°): C1–C1', 1.323(3); C1–C2, 1.466(2); C2–C1–C1'–C2, 180.0; C2–C7–C8–C13, –68.95(18).

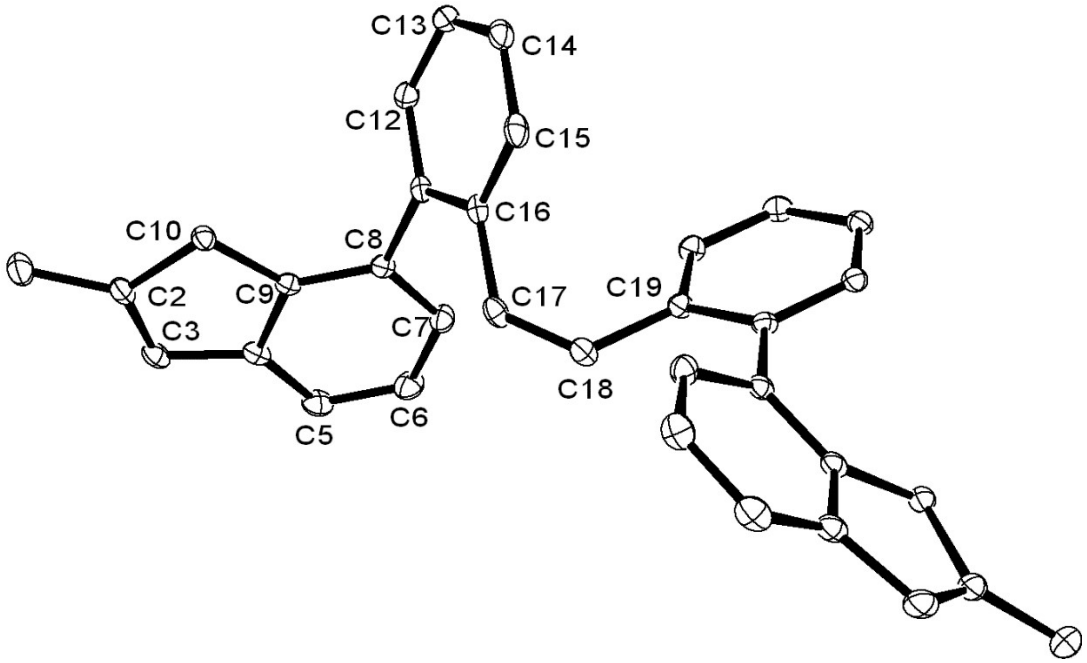

Figure S9. ORTEP plot of the solid-state molecular structure of {*o*-(*Z*)-BisIndSB}H_2 (ellipsoids set at 50% probability level; all H atoms omitted for clarity). Selected bond distances (Å) and angles (°): C17–C18, 1.332(2); C16–C17, 1.485(2); C16–C17–C18–C19, –9.8(2); C16–C11–C8–C9, 112.22(15).

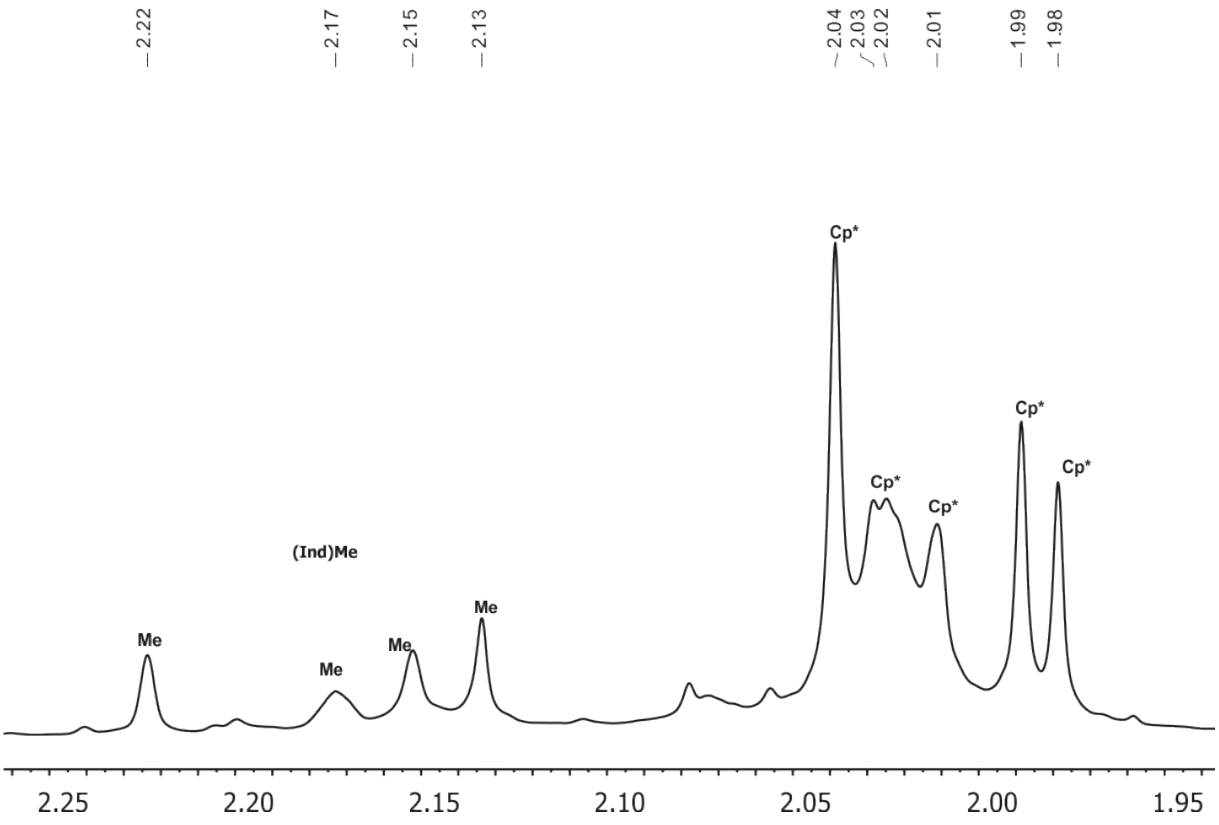

Figure S10. Detail of the aliphatic region of the ^{1}H NMR spectrum (400 MHz, $CDCl_3$, 23 °C) of {*o*-(*Z*)-BisIndSB}($ZrCl_2Cp^*)_2$.

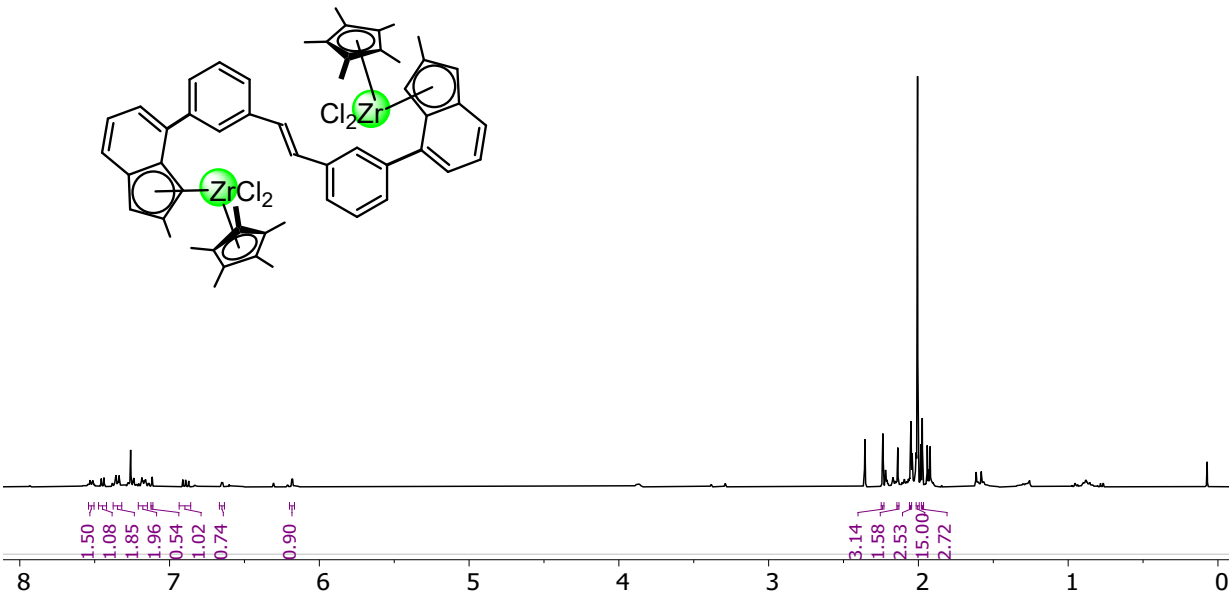

Figure S11. ^{1}H NMR spectrum (400 MHz, $CDCl_3$, 23 °C) of {*m*-(*E*)-BisIndSB}($ZrCl_2Cp^*)_2$.

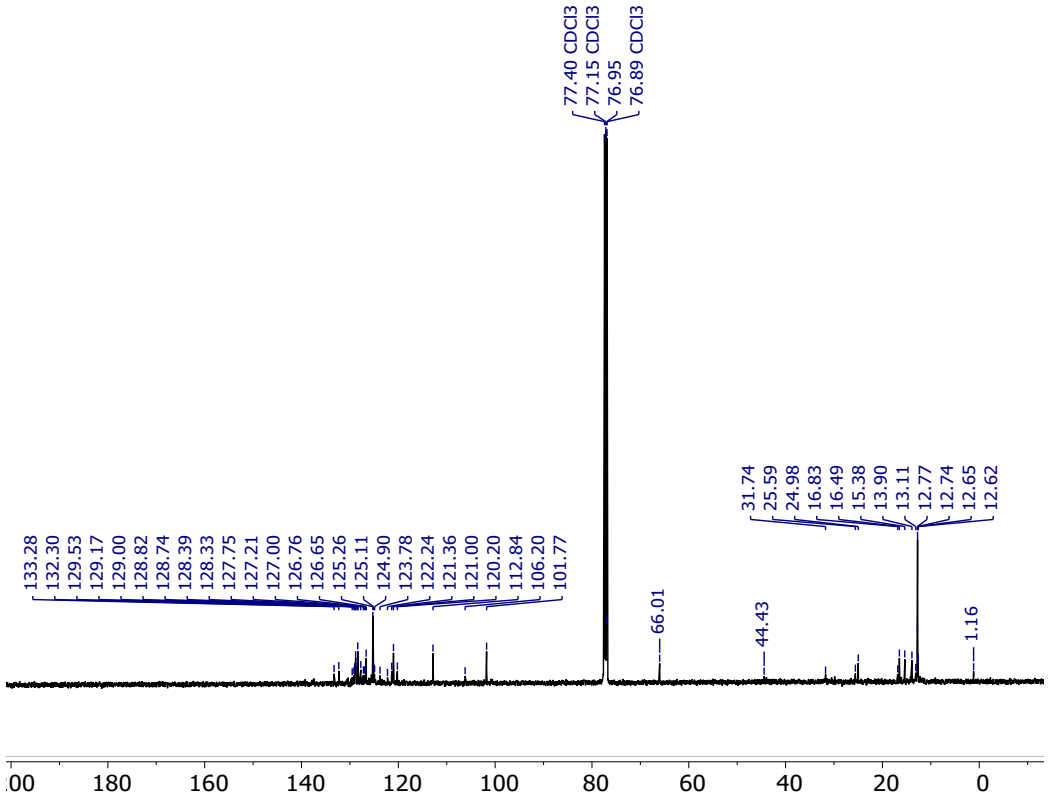

Figure S12. $^{13}C\{^{1}H\}$ NMR spectrum (101 MHz, $CDCl_3$, 23 °C) of {*m*-(*E*)-BisIndSB}($ZrCl_2Cp^*)_2$.

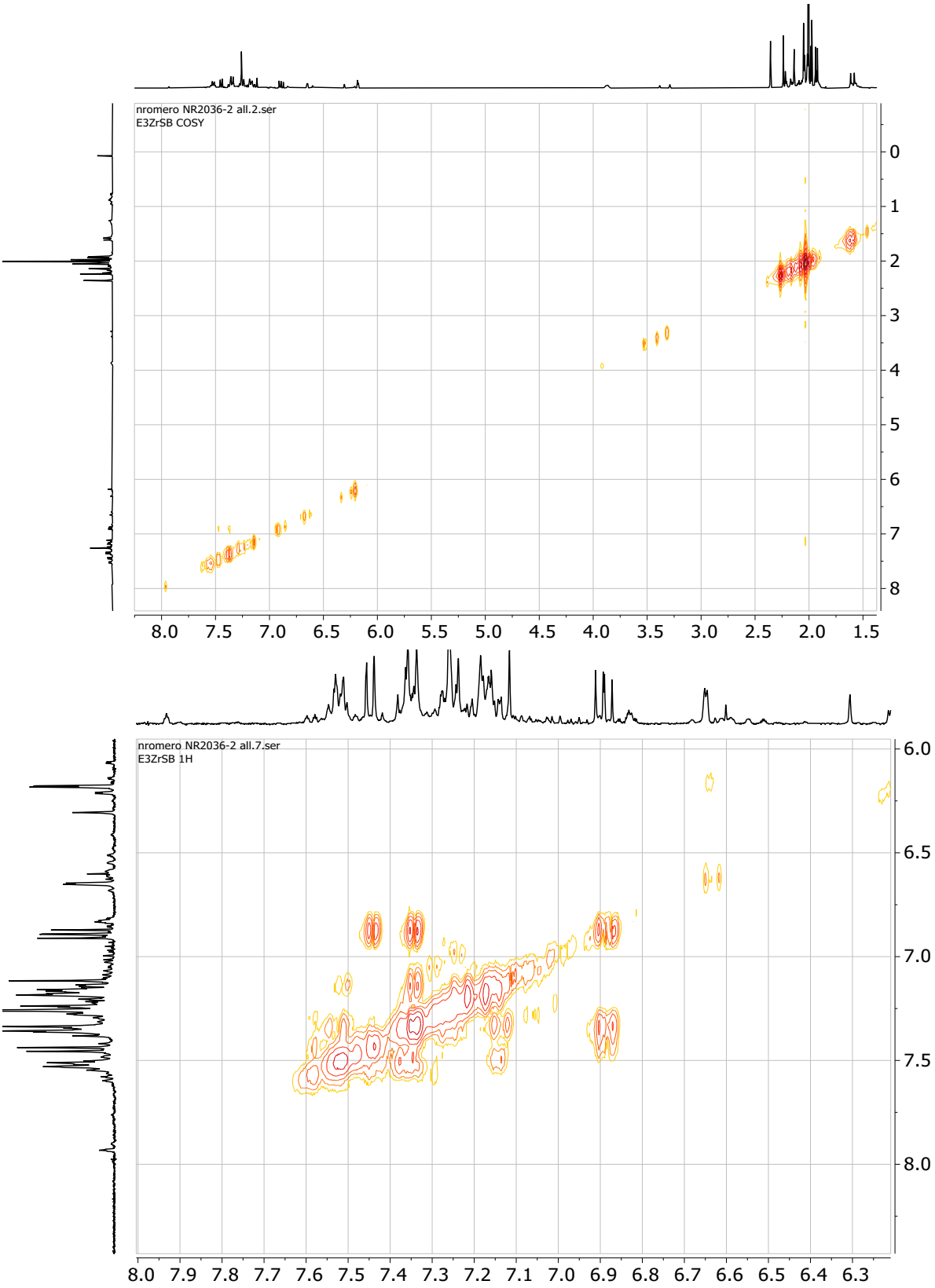

Figure S13. ^{1}H-^{1}H COSY NMR spectrum (400 MHz, $CDCl_3$, 23 °C) of {*m*-(*E*)-BisIndSB}$(ZrCl_2Cp^*)_2$.

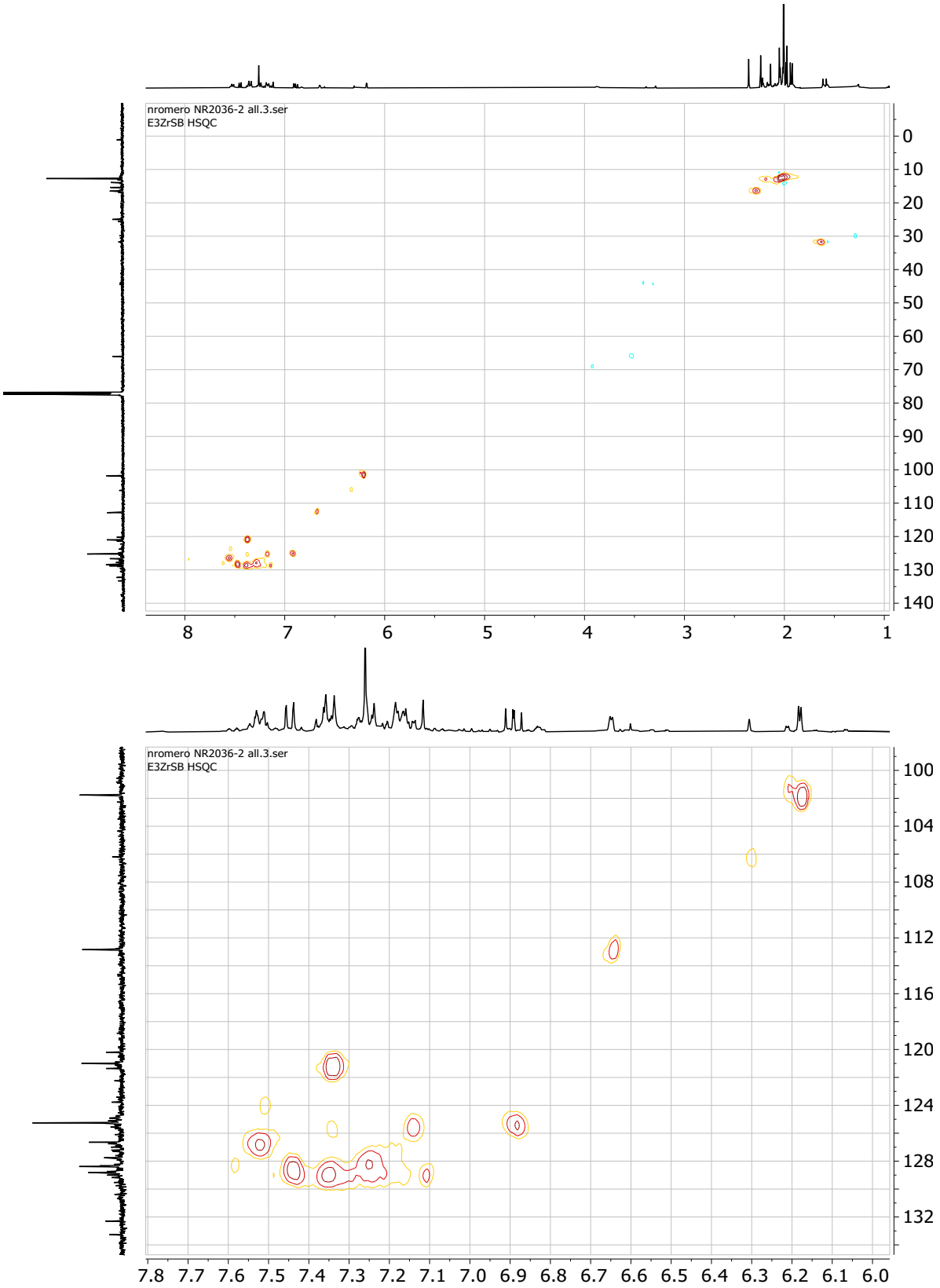

Figure S14. ^{1}H-^{13}C HSQC NMR spectrum (100 MHz, $CDCl_3$, 23 °C) of {*m*-(*E*)-BisIndSB}$(ZrCl_2Cp^*)_2$.

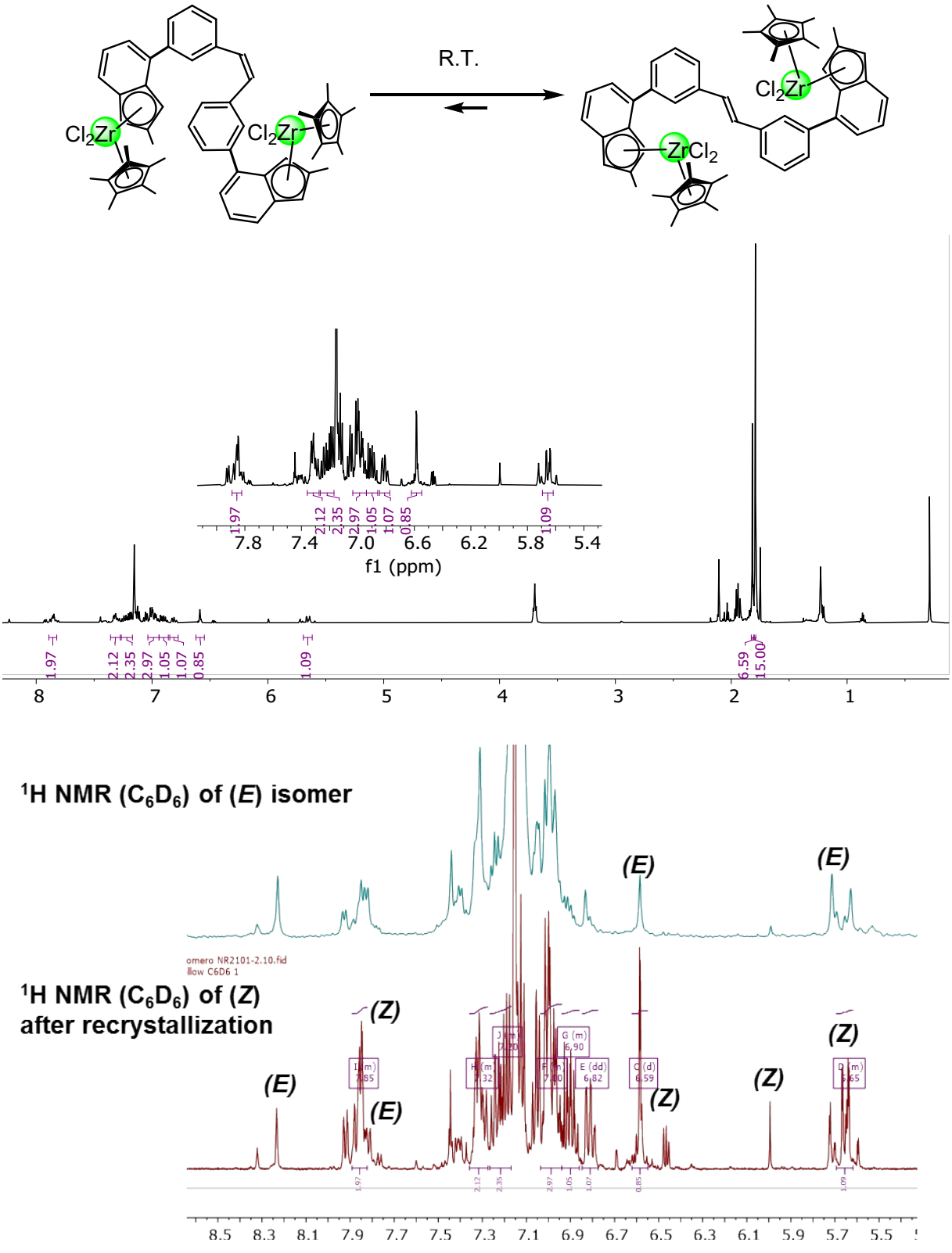

Figure S15. ^{1}H NMR spectra (400 MHz, C_6D_6, 23 °C) of (top): a mixture of *(Z)*- and (*E*)-{*m*-BisIndSB}($ZrCl_2Cp^*)_2$ obtained after recrystallization of the reaction mixture and (bottom): comparison of the mixture with pure {*m*-*(E)*-BisIndSB}($ZrCl_2Cp^*)_2$.

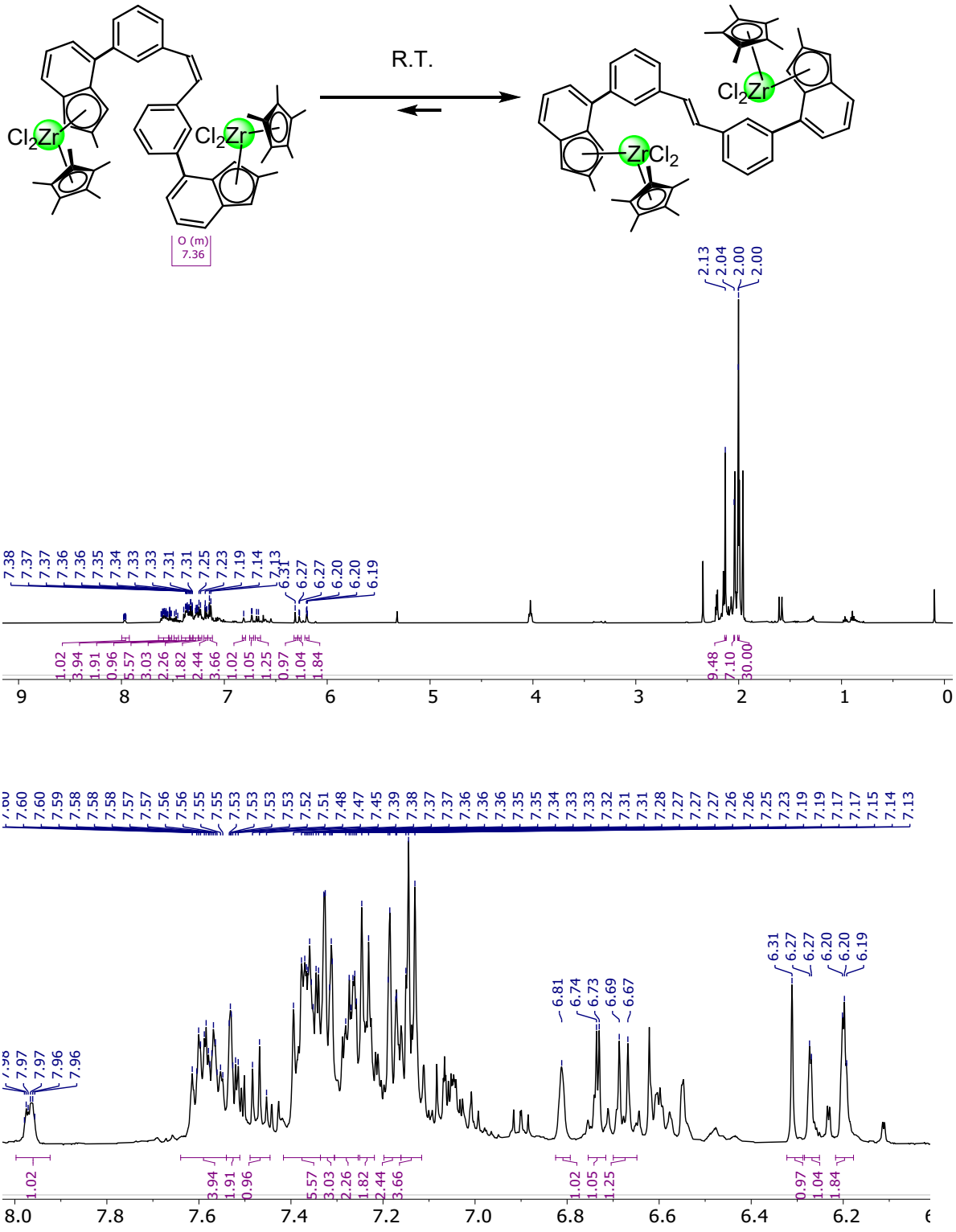

Figure S16. ^{1}H NMR spectrum (400 MHz, CD_2Cl_2, 23 °C) of a mixture of (*Z*)- and (*E*)-{*m*-{BisIndSB}($ZrCl_2Cp^*$)$_2$.

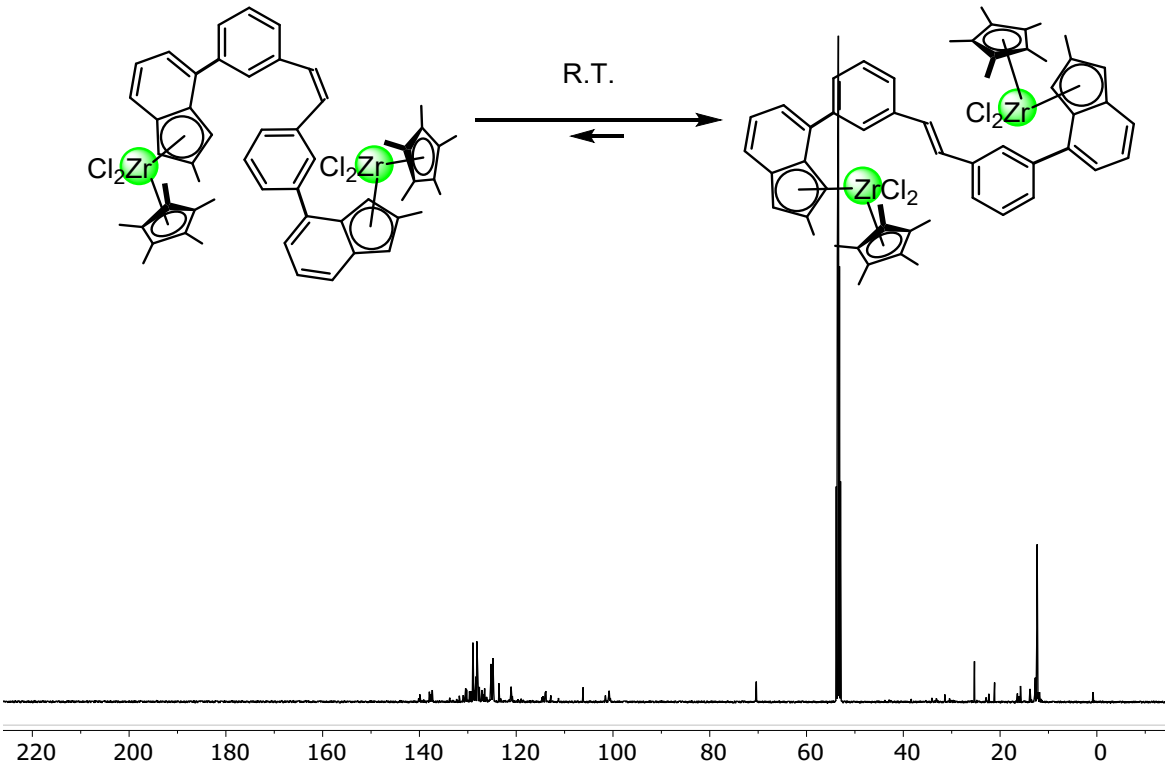

Figure S17. $^{13}C\{^{1}H\}$ NMR spectrum (101 MHz, CD_2Cl_2, 23 °C) of a mixture of (*Z*)- and (*E*)-*m*-{BisIndSB}($ZrCl_2Cp^*)_2$.

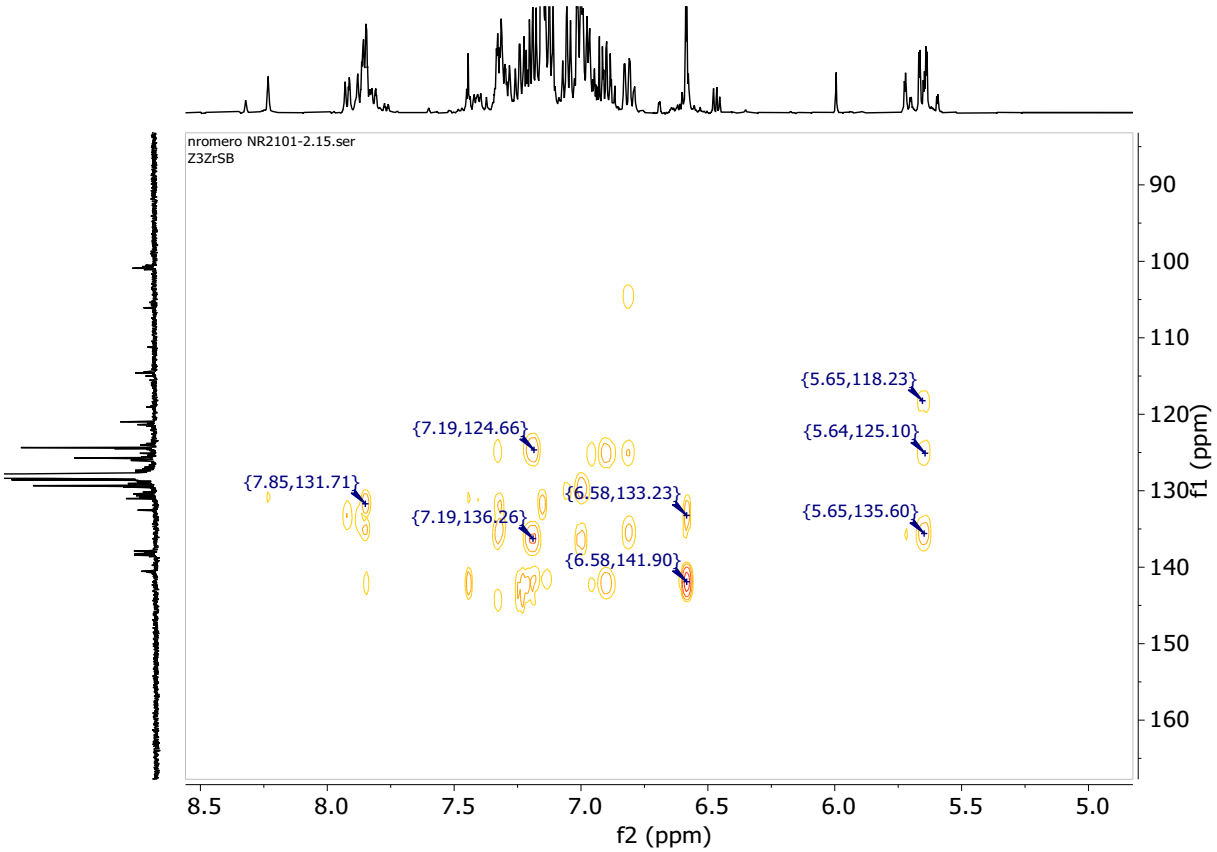

Figure S18. ^{1}H-^{13}C HSQC NMR spectrum (100 MHz, CD_2Cl_2, 23 °C) of a mixture of (*Z*)- and (*E*)-*m*-{BisIndSB}($ZrCl_2Cp^*)_2$.

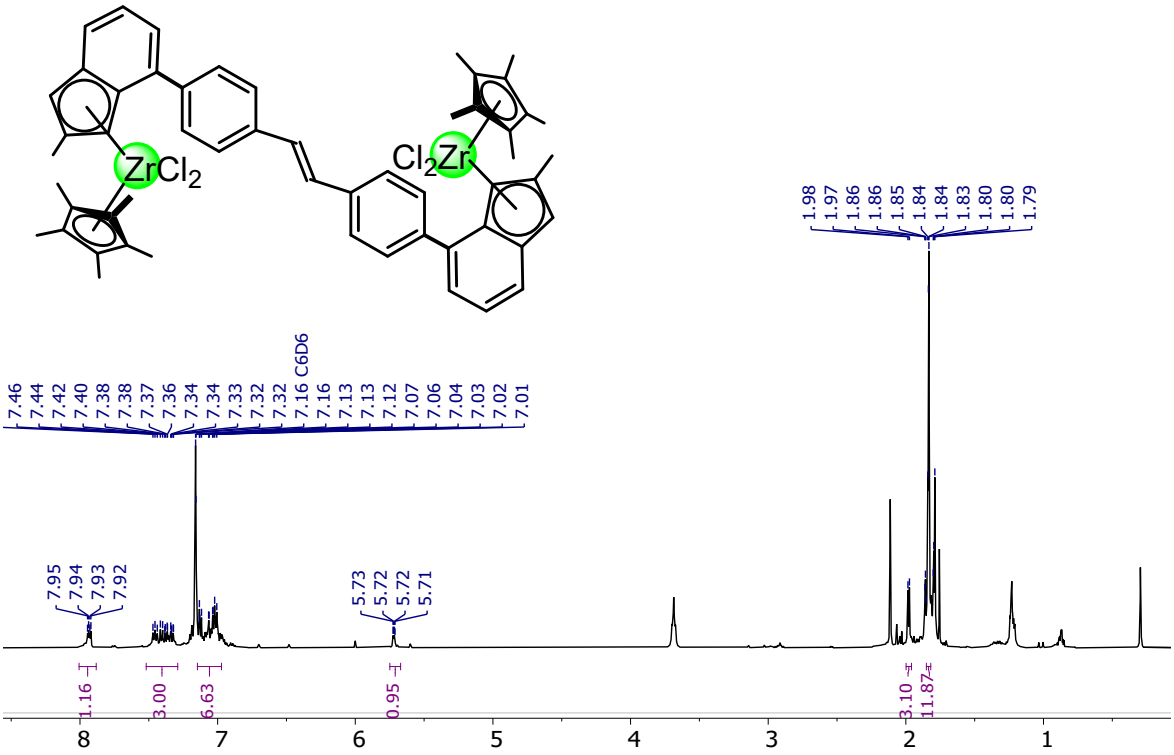

Figure S19. ^{1}H NMR spectrum (400 MHz, C_6D_6, 23 °C) of {*p*-(*E*)-BisIndSB}($ZrCl_2Cp^*)_2$.

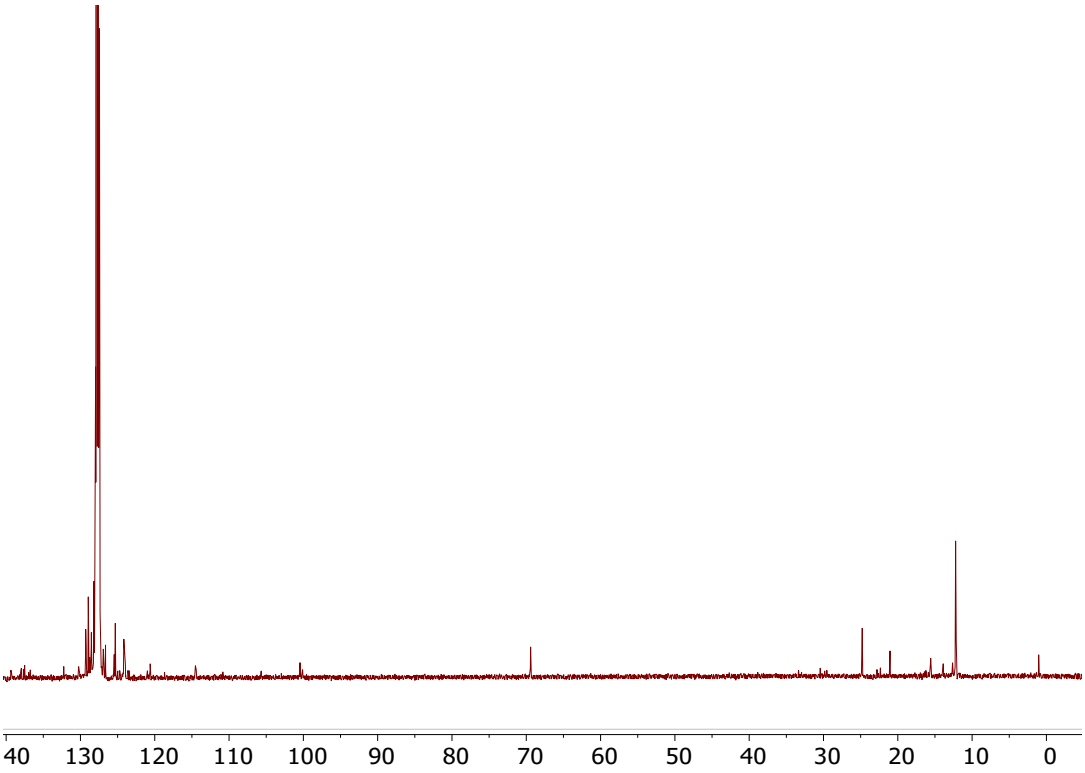

Figure S20. $^{13}C\{^{1}H\}$ NMR spectrum (101 MHz, C_6D_6, 23 °C) of {*p*-(*E*)-BisIndSB}($ZrCl_2Cp^*)_2$.

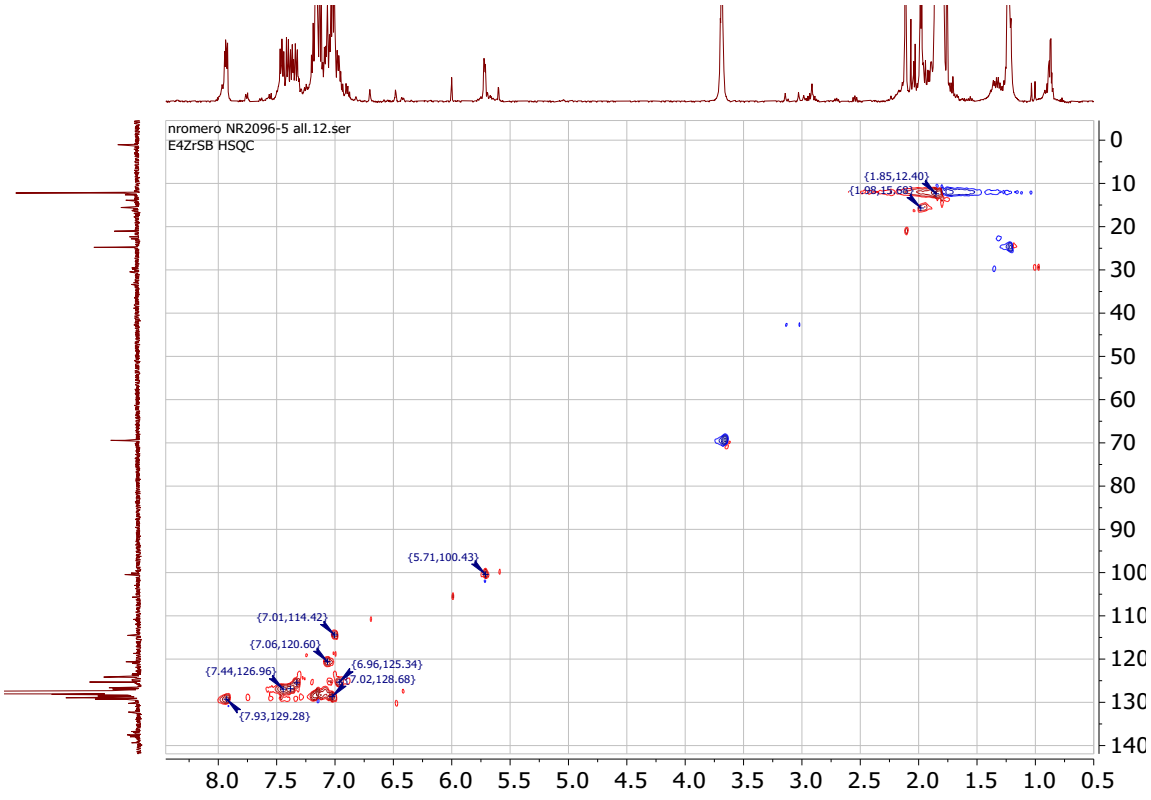

Figure S21. ^{1}H-^{13}C HSQC NMR spectrum (100 MHz, C_6D_6, 23 °C) of {*p*-(*E*)-BisInd}($ZrCl_2Cp^*)_2$.

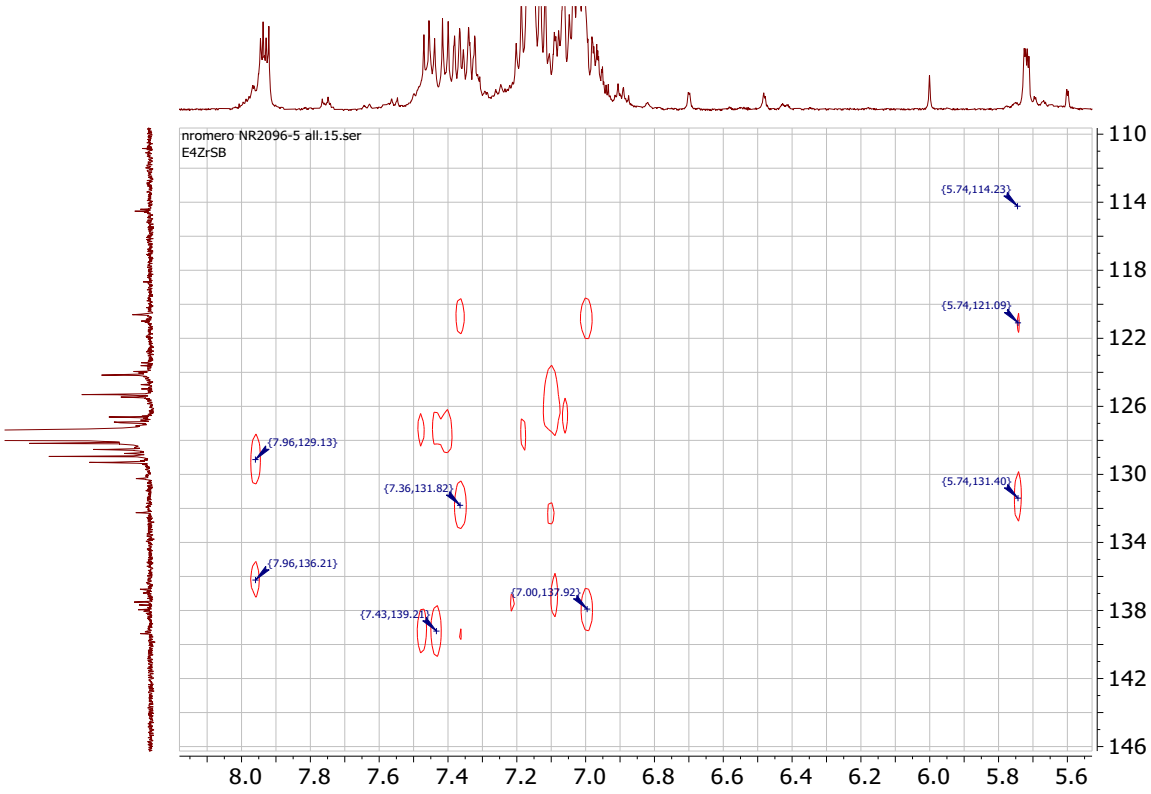

Figure S22. ^{1}H-^{13}C HMBC NMR spectrum (400 MHz, C_6D_6, 23 °C) of {*p*-(*E*)-BisInd}($ZrCl_2Cp^*)_2$.

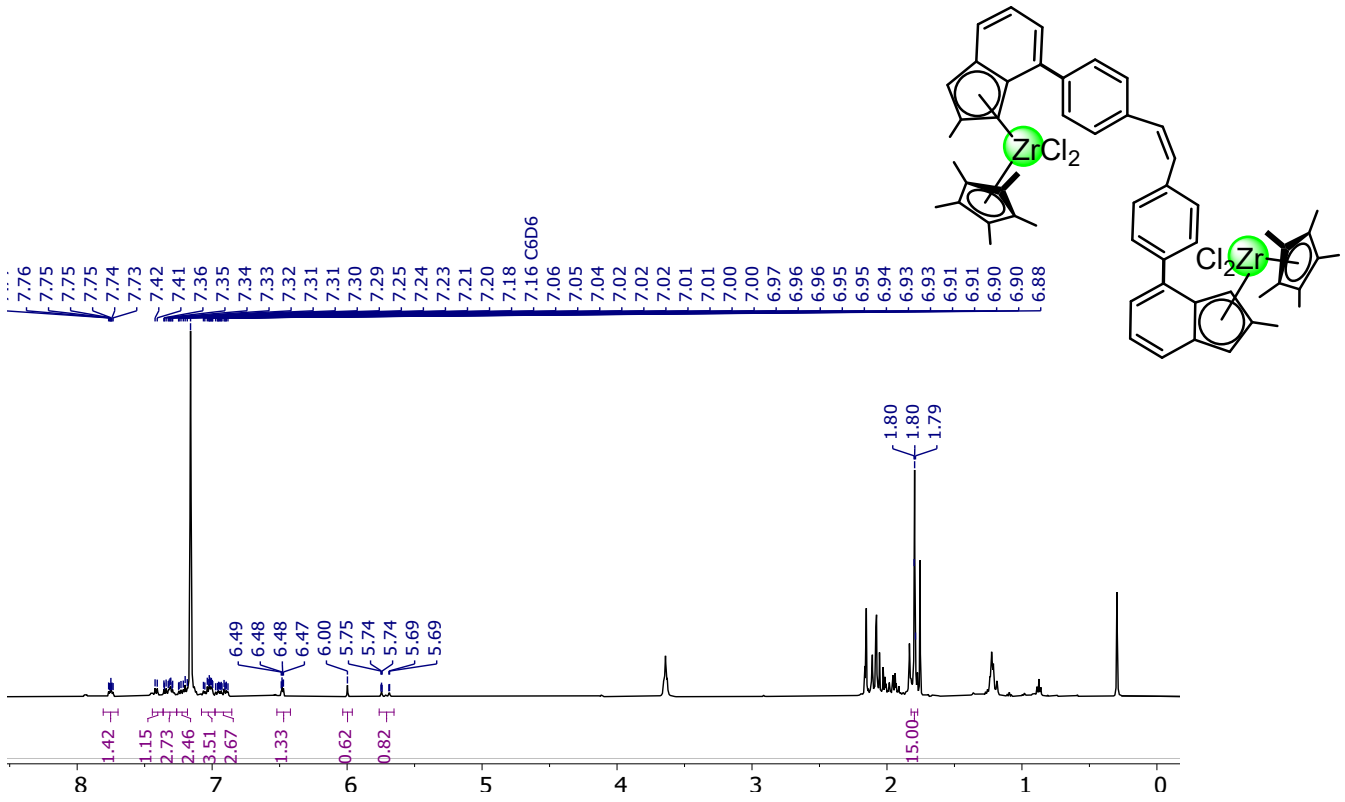

Figure S23. ^{1}H NMR spectrum (400 MHz, C_6D_6, 23 °C) of {*p*-(*Z*)-BisIndSB}($ZrCl_2Cp^*)_2$.

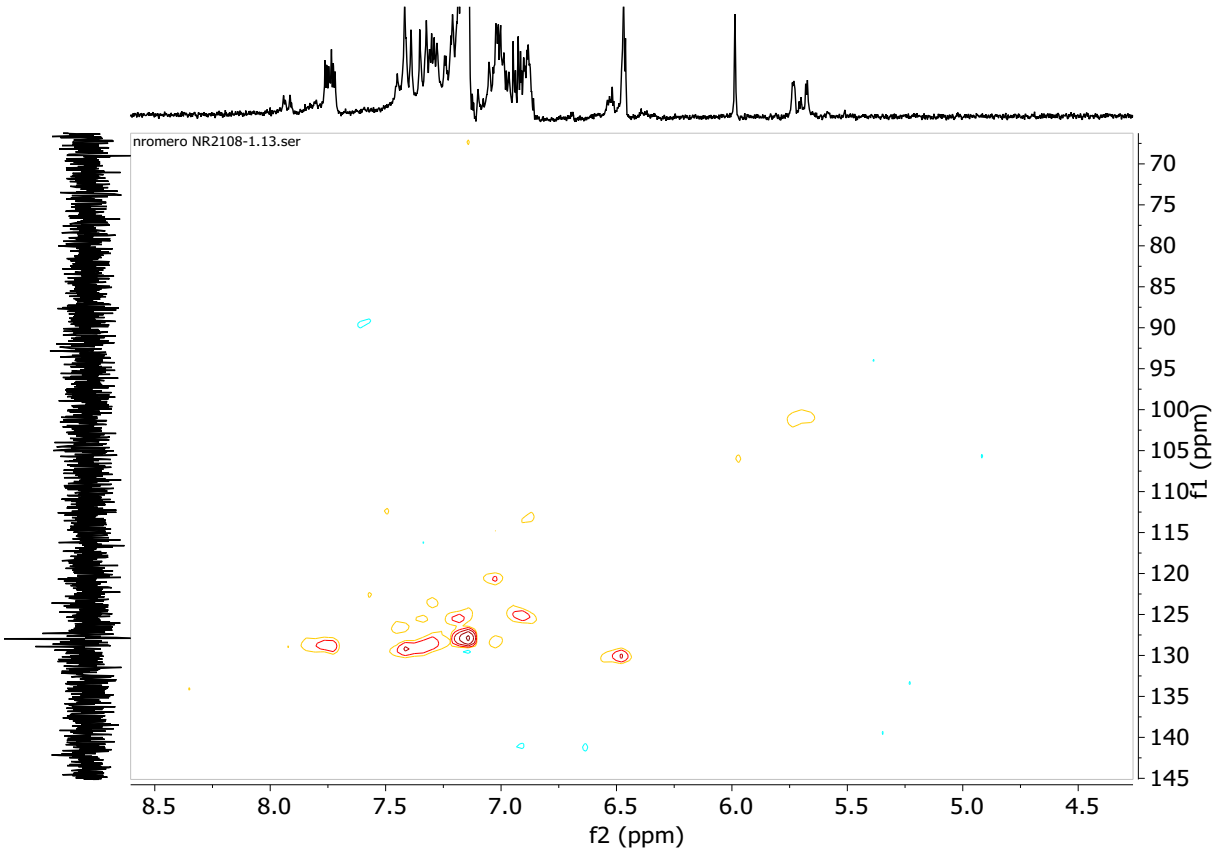

Figure S24. ^{1}H-^{13}C HSQC NMR spectrum (100 MHz, C_6D_6, 23 °C) of {*p*-(*Z*)-BisIndSB}($ZrCl_2Cp^*)_2$.

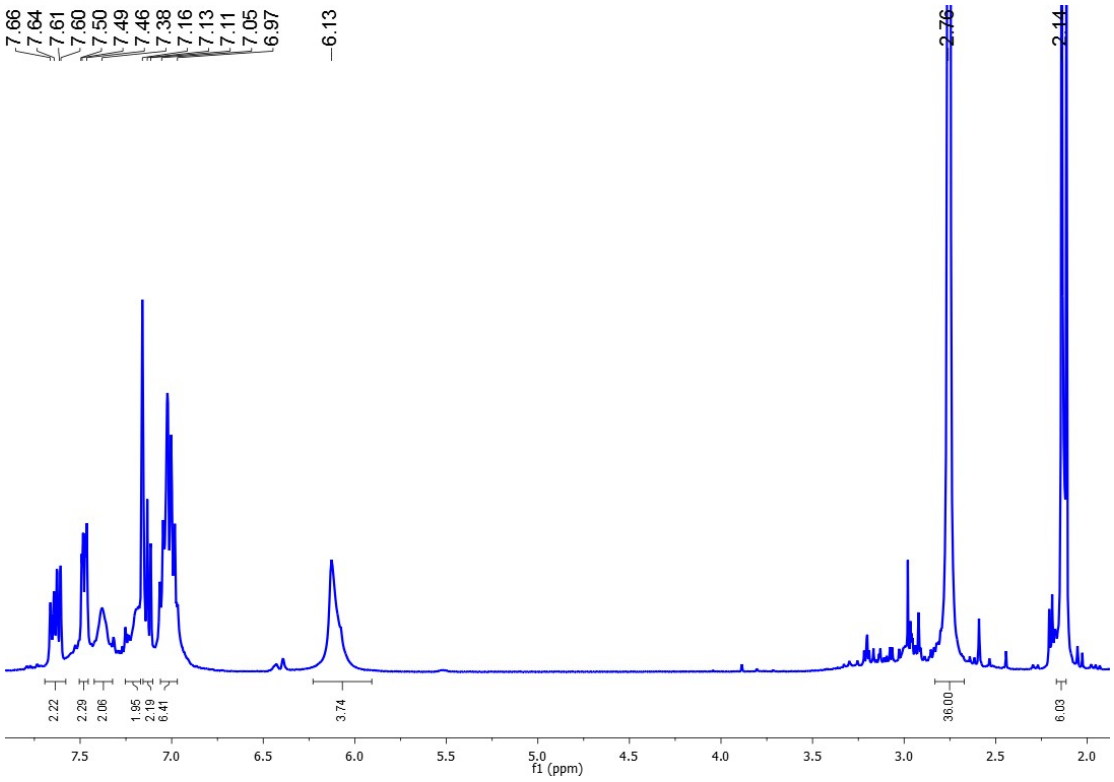

Figure S25. ^{1}H NMR spectrum (400 MHz, C_6D_6, 25 °C) of *o*-(*E*)-BisIndSB}(Zr(NMe$_2$)$_3$)$_2$.

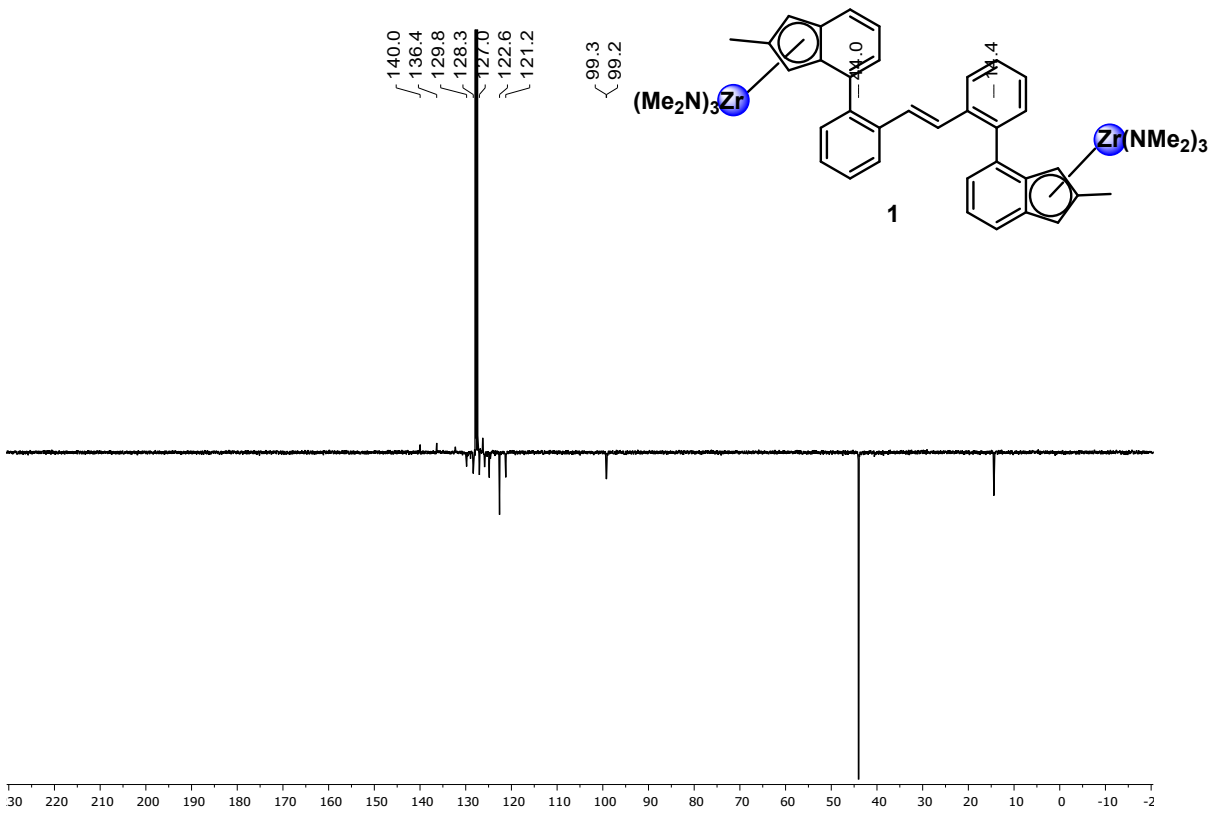

Figure S26. ^{13}C{^{1}H} JMOD NMR spectrum (101 MHz, C_6D_6, 23 °C) of *o*-(*E*)-BisIndSB}(Zr(NMe$_2$)$_3$)$_2$.

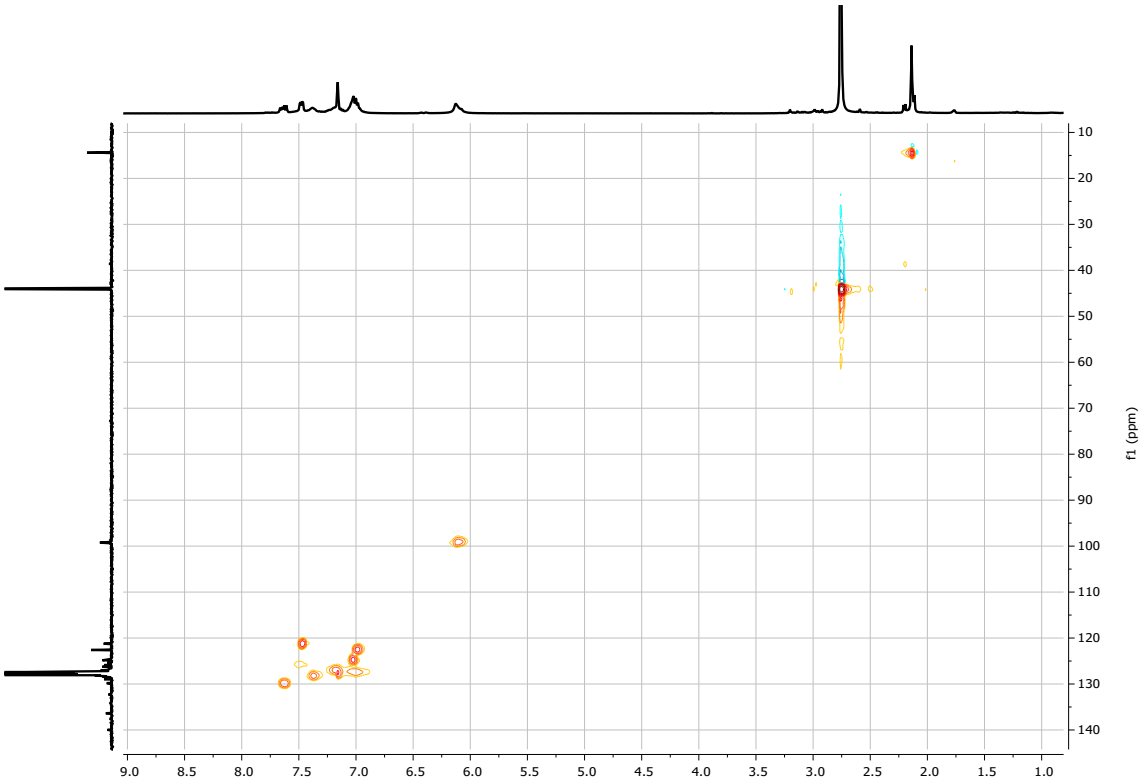

Figure S27. ^{1}H-^{13}C HSQC NMR spectrum (100 MHz, C_6D_6, 25 °C) of {*o*-(*E*)-BisIndSB}$(Zr(NMe_2)_3)_2$.

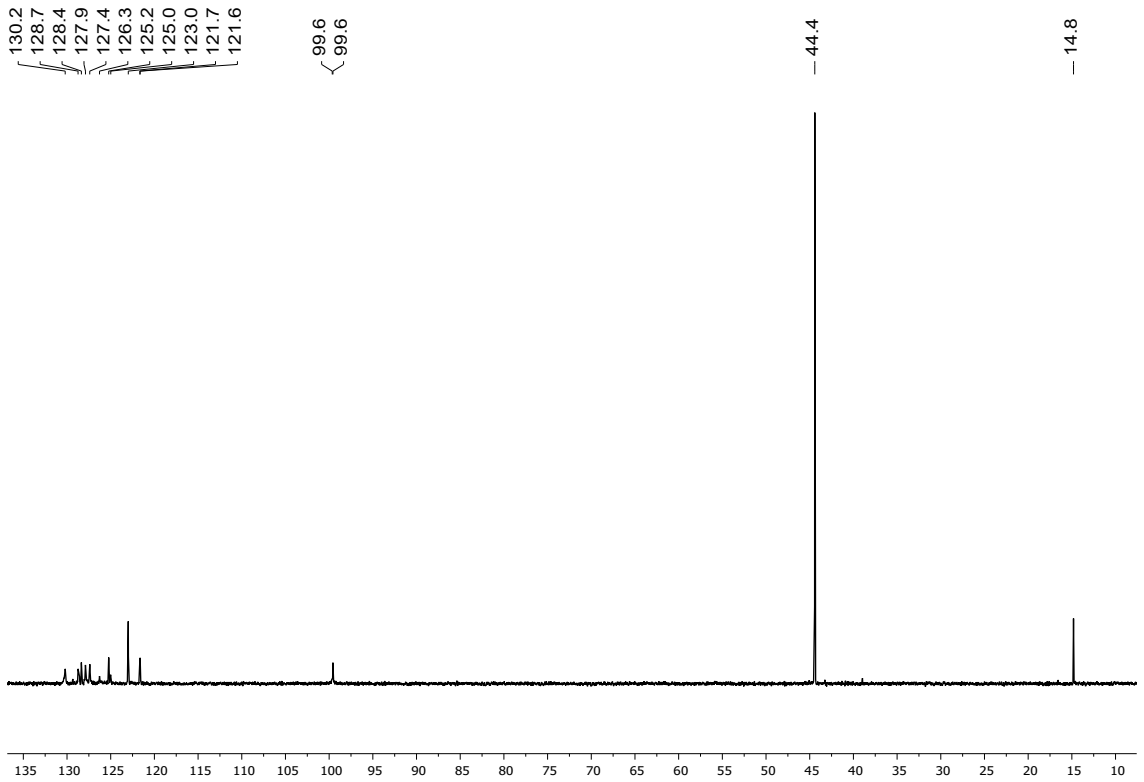

Figure S28. DEPT 135 ^{13}C NMR spectrum (101 MHz, C_6D_6, 25 °C) of {*o*-(*E*)-BisIndSB}$(Zr(NMe_2)_3)_2$.

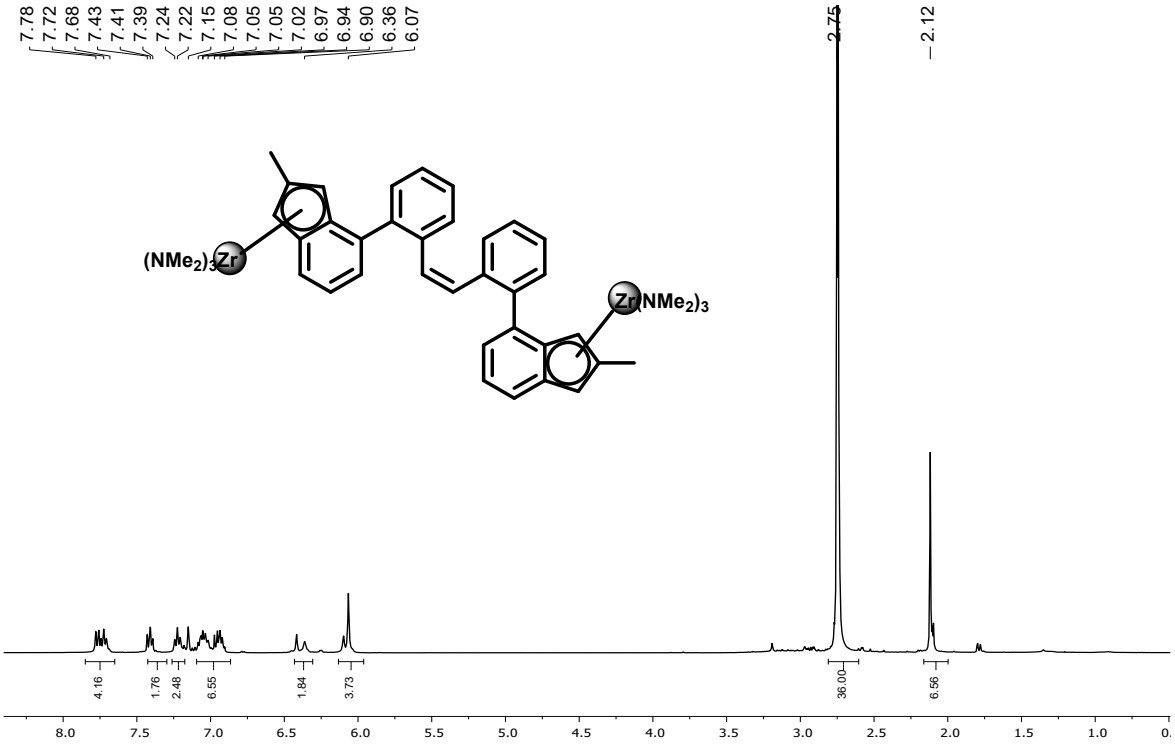

Figure S29. ^{1}H NMR spectrum (400 MHz, C_6D_6, 23 °C) of {*o*-(*Z*)-BisIndSB}($Zr(NMe_2)_3)_2$.

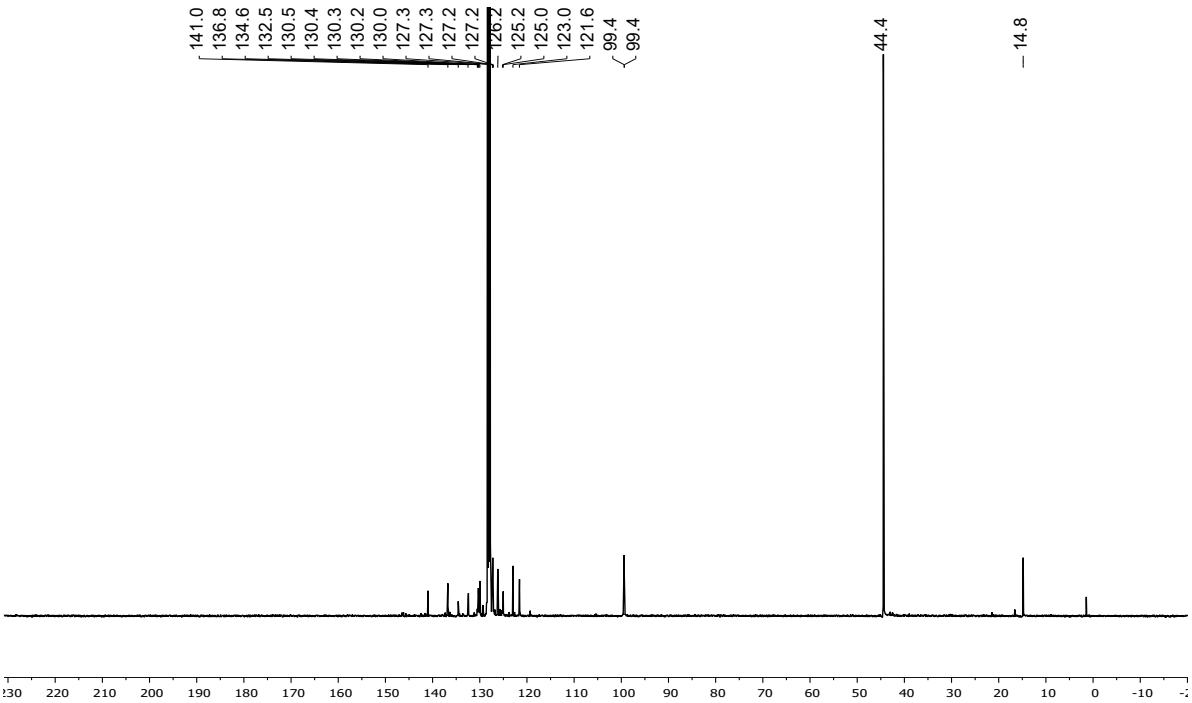

Figure S30. $^{13}C\{^{1}H\}$ NMR spectrum (101 MHz, C_6D_6, 25 °C) of {*o*-(*Z*)-BisIndSB}($Zr(NMe_2)_3)_2$.

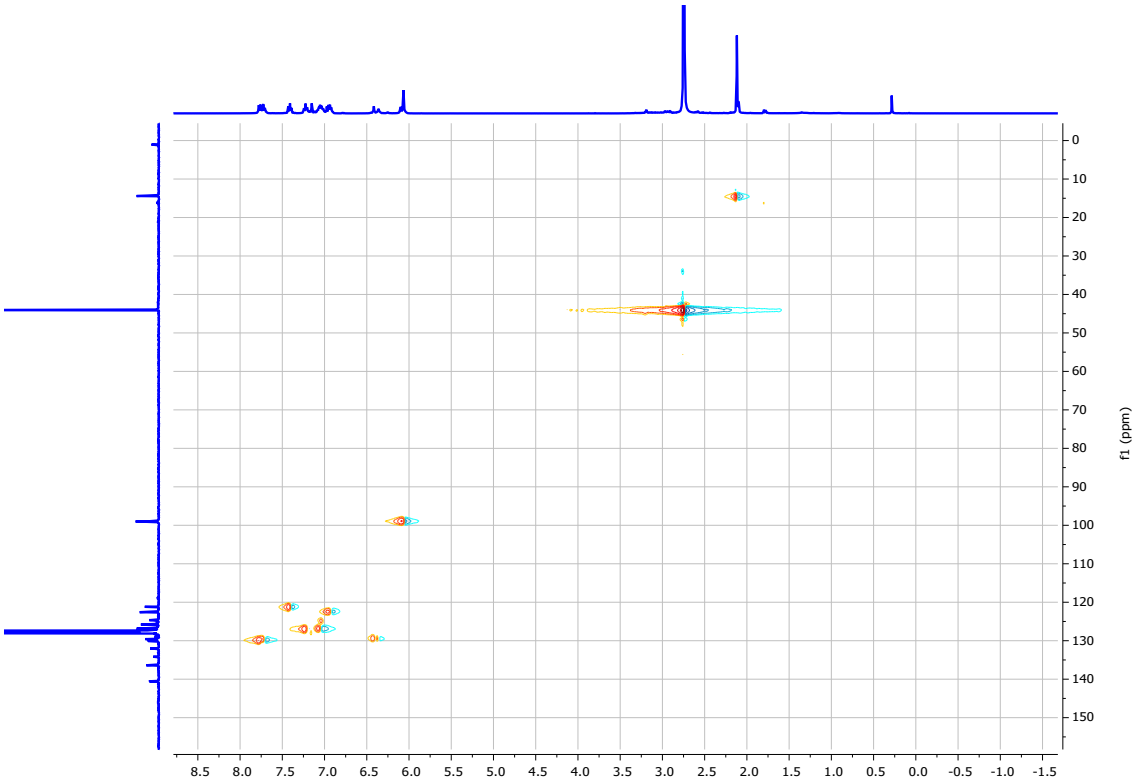

Figure S31. ^{1}H-^{13}C HSQC NMR spectrum (100 MHz, C_6D_6, 25 °C) of {*o*-(*Z*)-BisIndSB}$(Zr(NMe_2)_3)_2$.

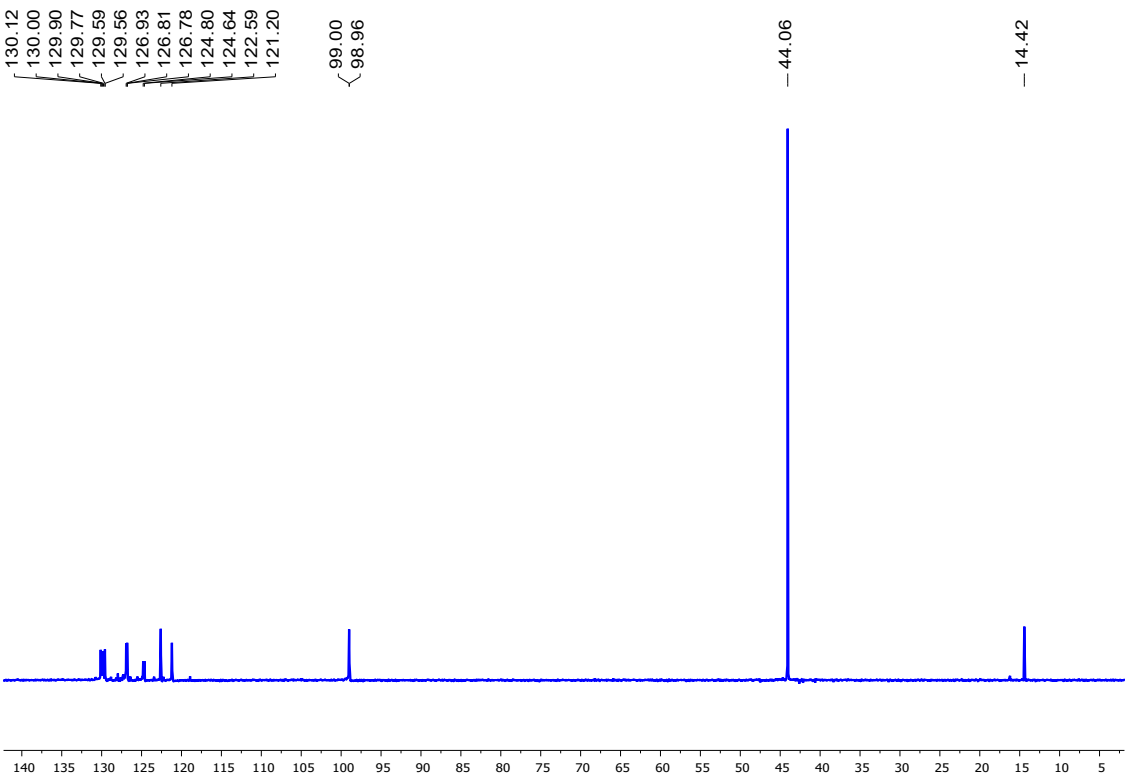

Figure S32. DEPT 135 ^{13}C NMR spectrum (101 MHz, C_6D_6, 23 °C) of {*o*-(*Z*)-BisIndSB}$(Zr(NMe_2)_3)_2$.

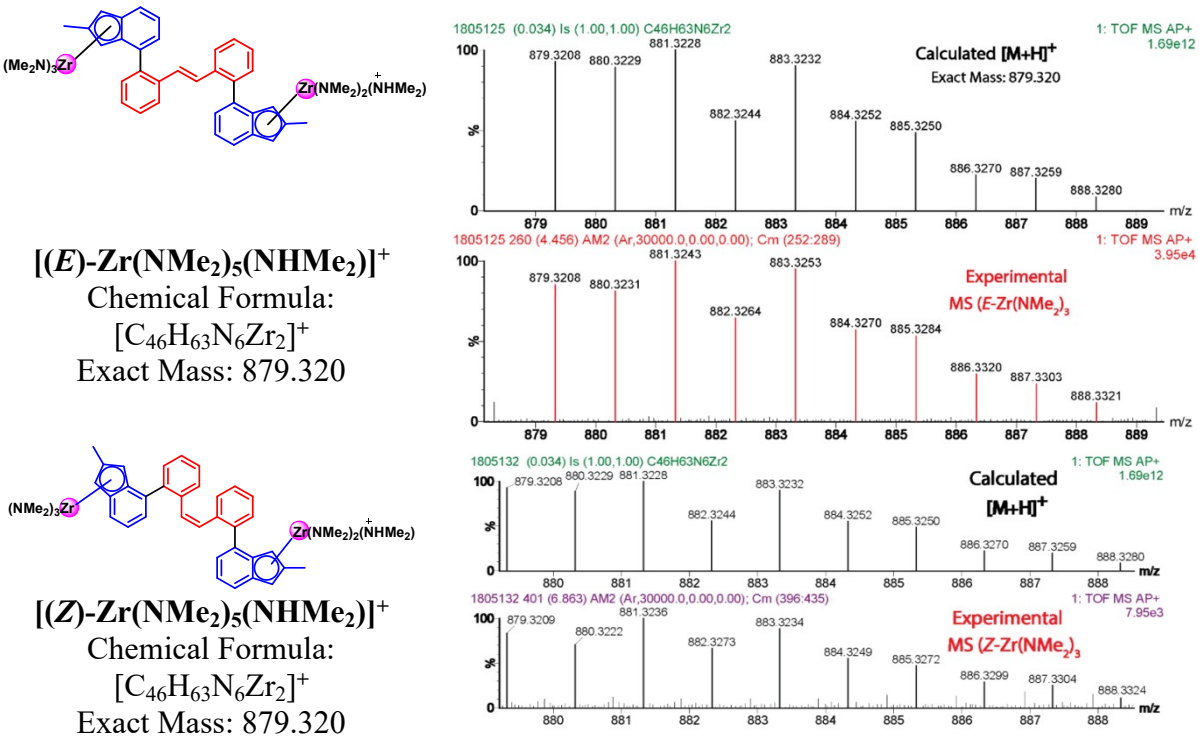

Figure S33. Inert Atmospheric Solid Analysis Probe (iASAP) data for complexes {*o*-(*E*/*Z*)-BisIndSB}$(Zr(NMe_2)_3)_2$.

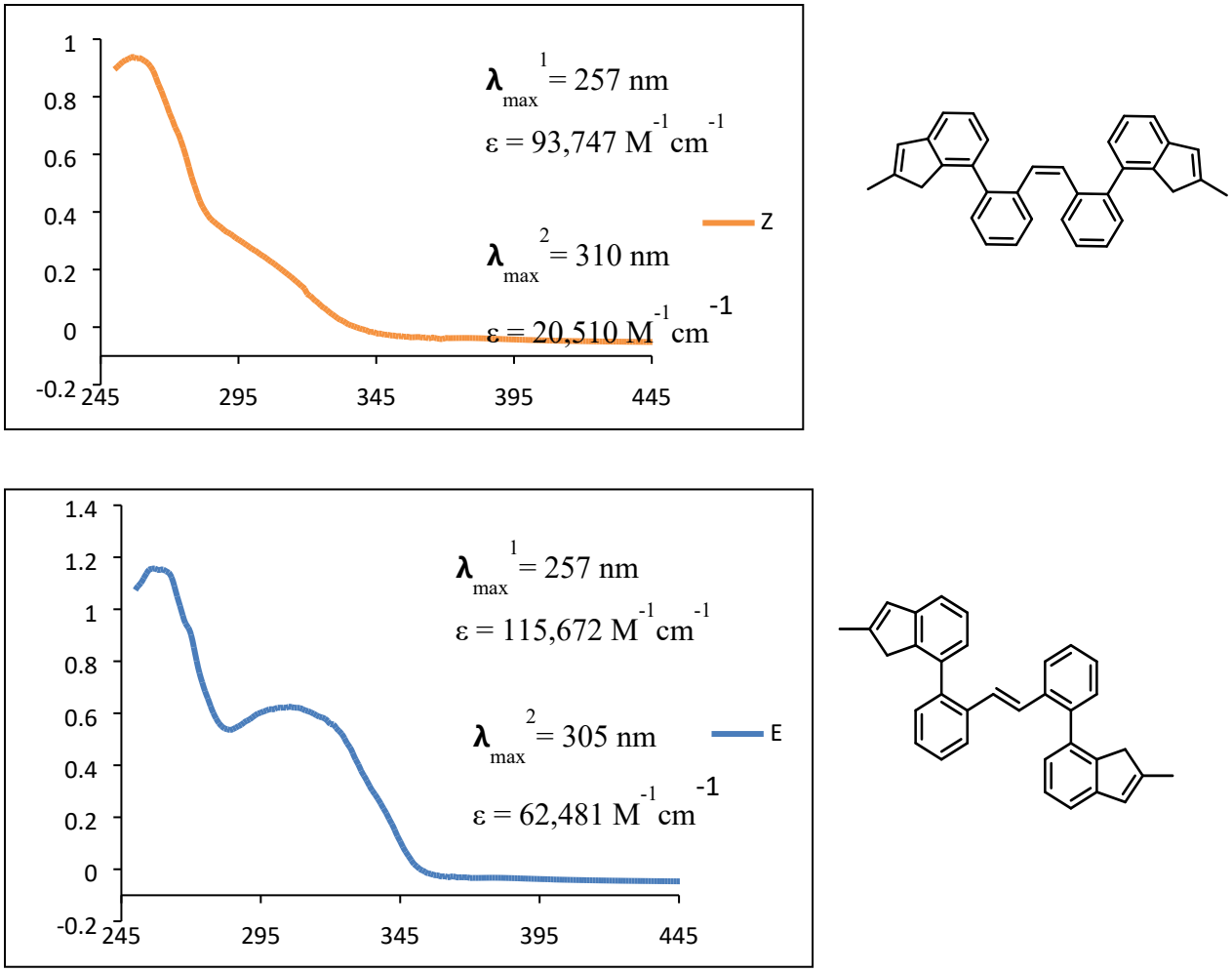

Figure S34. Absorption spectra of {*o*-(*Z*)-BisIndSB}H_2 and {*o*-(*E*)-BisIndSB}H_2 proligands in CH_2Cl_2 at 10^{-5} M.

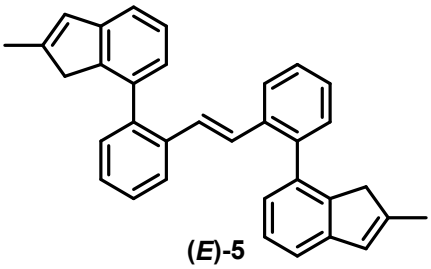

(*E*)-5

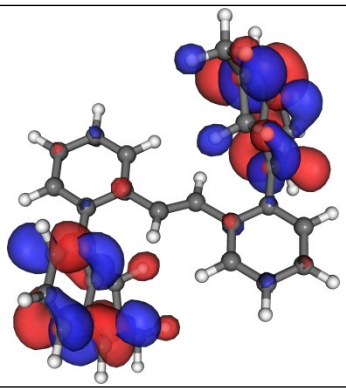	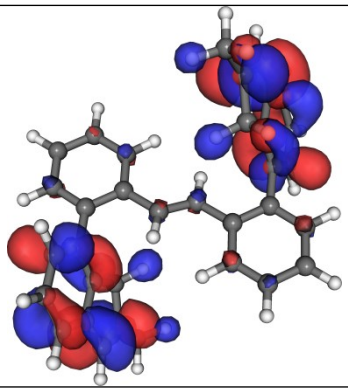
LUMO+1	LUMO+2
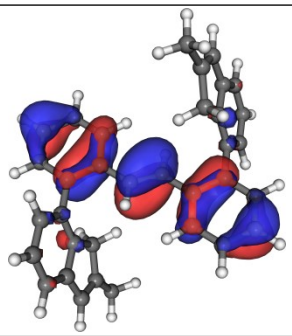	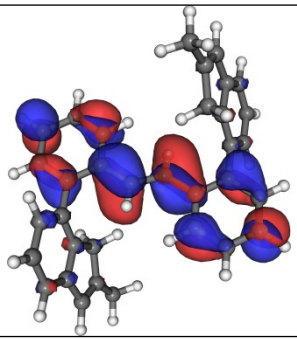
HOMO	LUMO
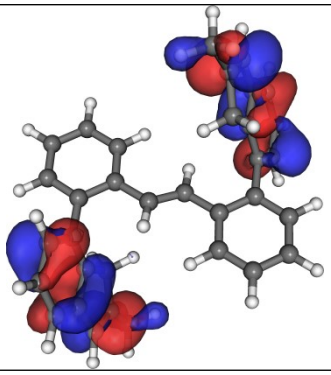	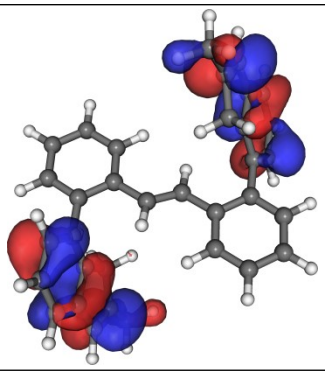
HOMO-2	HOMO-1

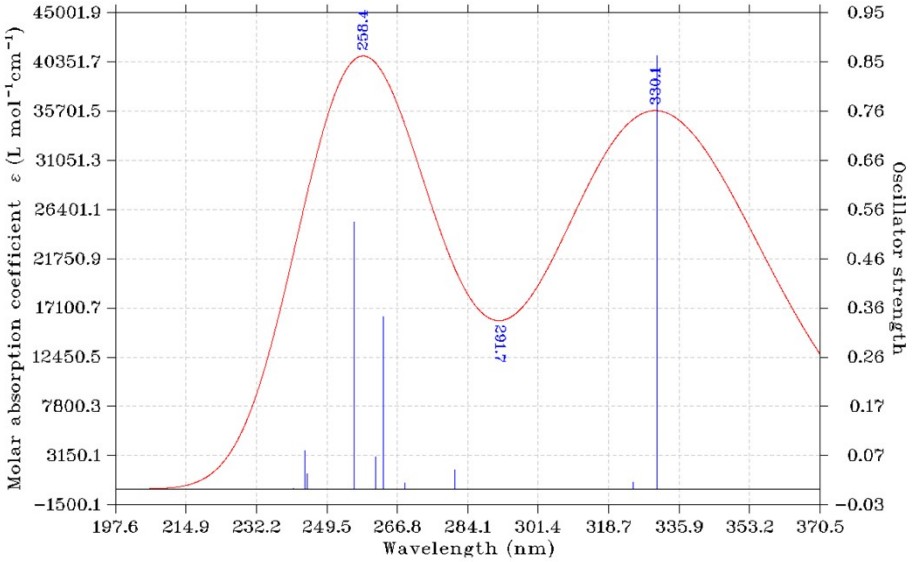

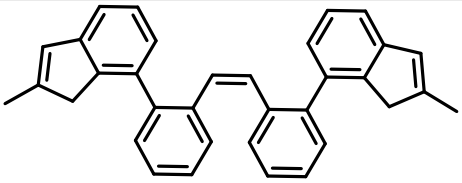

(Z)-5

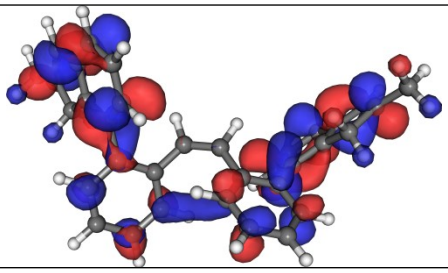

LUMO+1

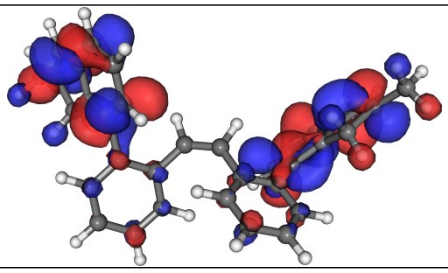

LUMO+2

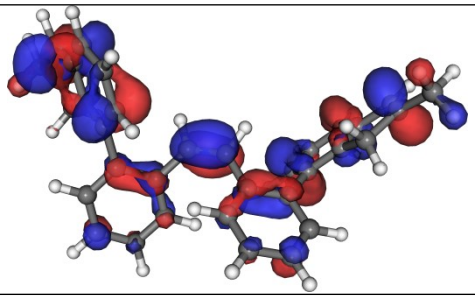

HOMO

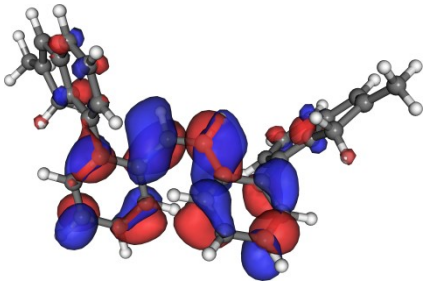

LUMO

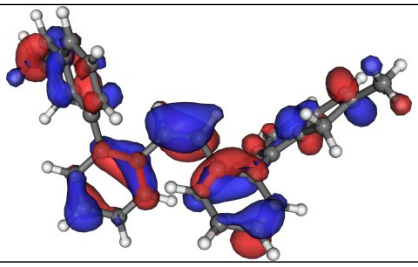

HOMO-2

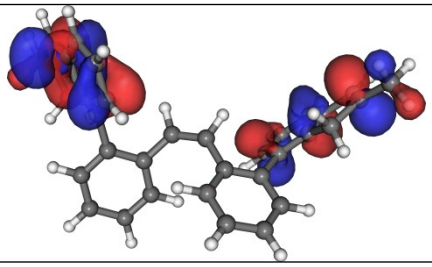

HOMO-1

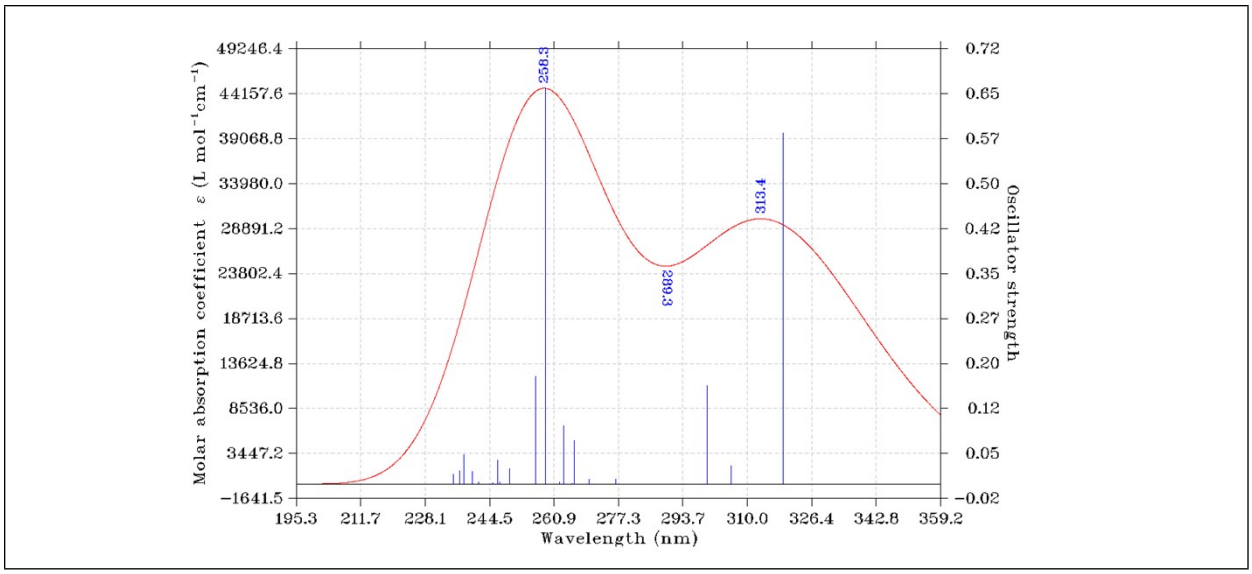

Figure S35. Frontier Kohn-Sham orbitals and absorption spectra calculated for {*o*-(*Z*/*E*)-BisIndSB}H_2 proligands.

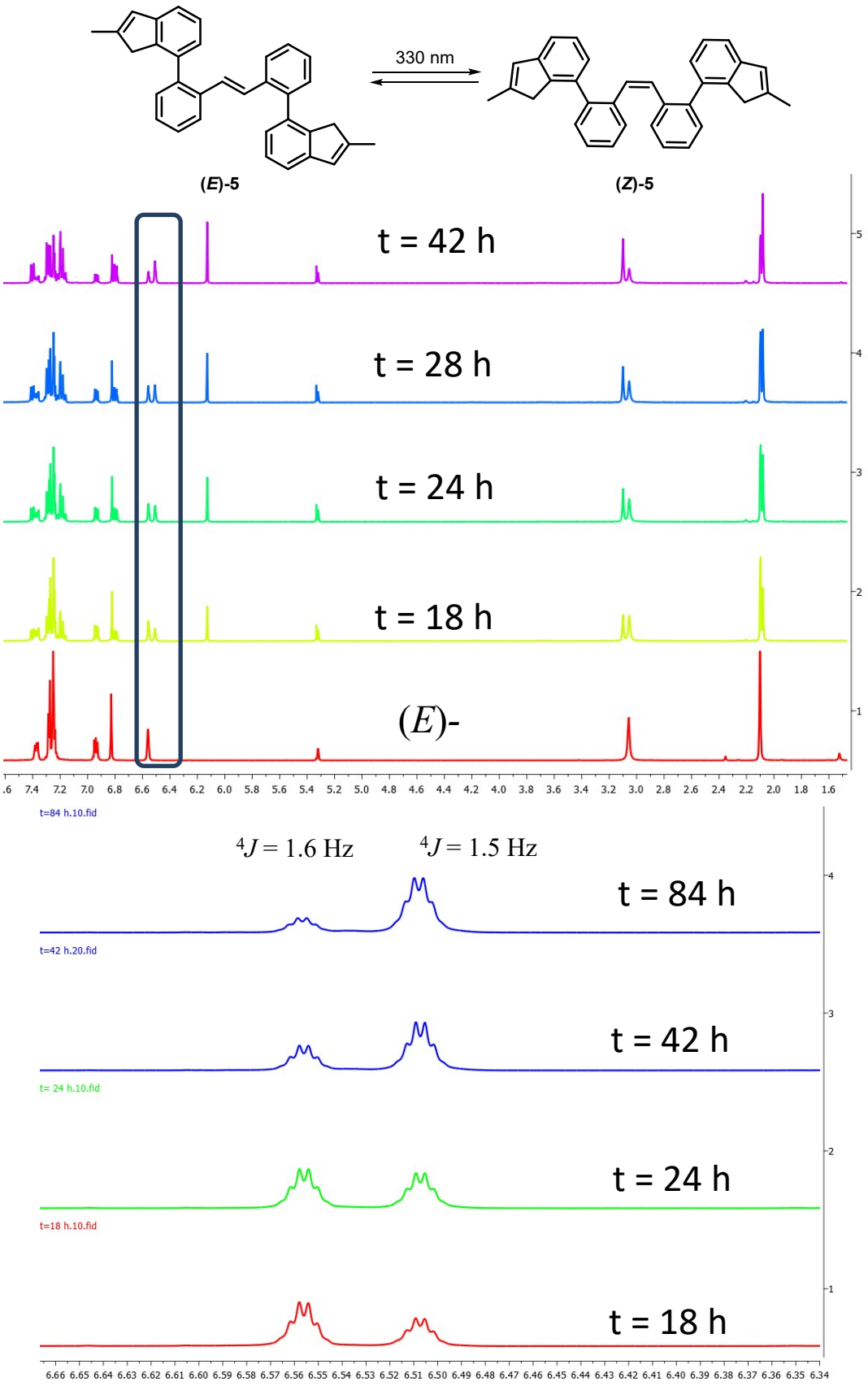

Figure S36. Photoisomerization of (*E*)- to (*Z*)-{BisIndSB}H_2 proligands by UV irradiation at λ = 330 nm, monitored by ^{1}H NMR in CD_2Cl_2 at 10^{-2} M, 23 °C.

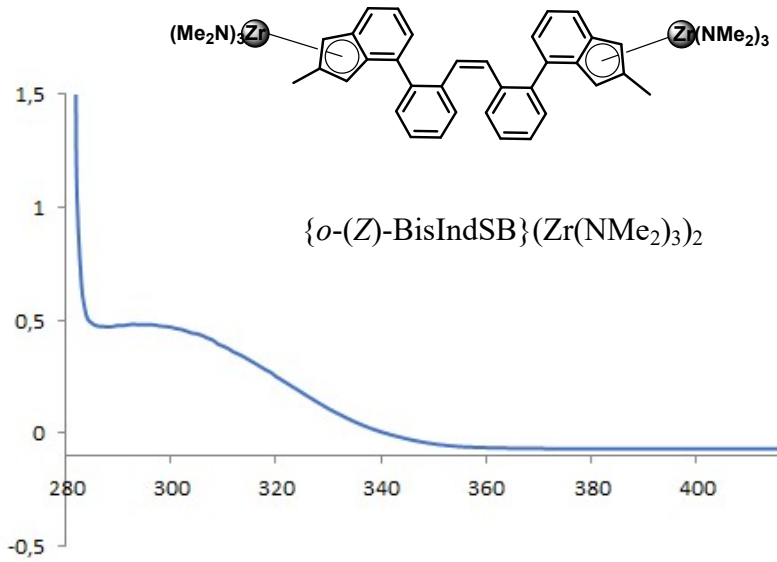

{*o*-(*Z*)-BisIndSB}(Zr(NMe$_2$)$_3$)$_2$

Inflection point at 325 nm

λ_{max}^{1} = 293 nm

ε= 96499 M^{-1}cm^{-1}

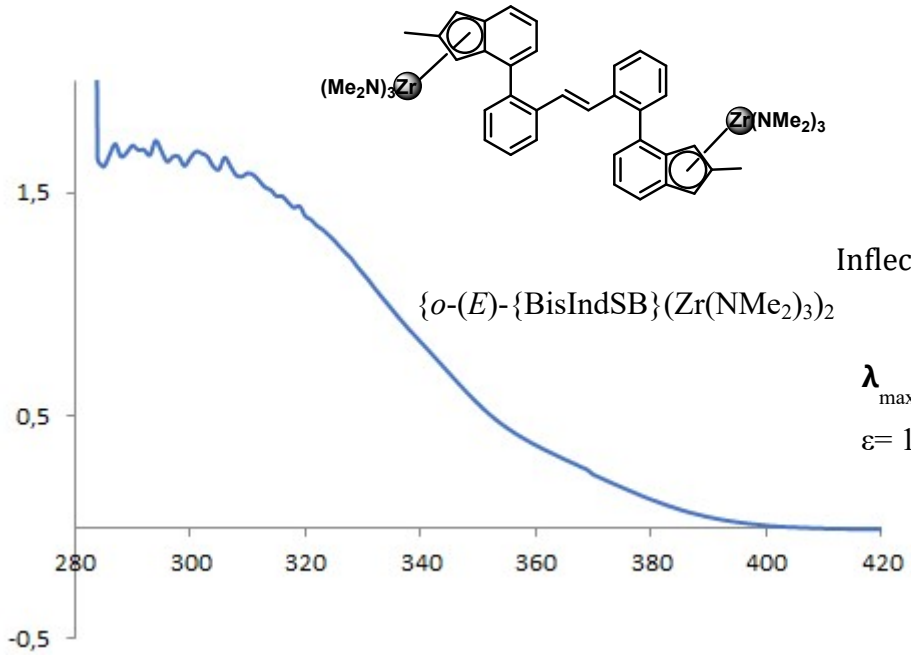

Inflection point at 340 nm

{*o*-(*E*)-{BisIndSB}(Zr(NMe$_2$)$_3$)$_2$

λ_{max}^{1} = 294 nm

ε= 173 000 M^{-1}cm^{-1}

Figure S37. Absorption spectra of (*Z*)- and (*E*)-{*o*-BisIndSB}(Zr(NMe$_2$)$_3$)$_2$ complexes in toluene at 10^{-5} M.

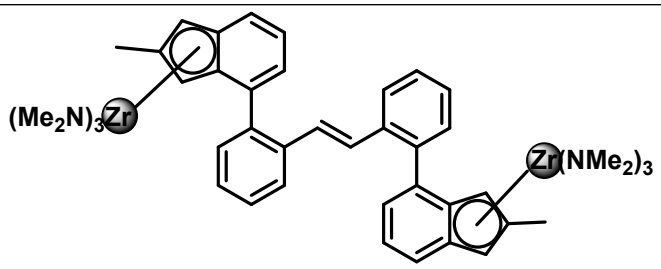

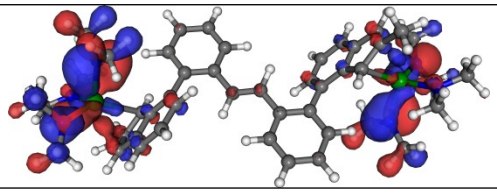

HOMO

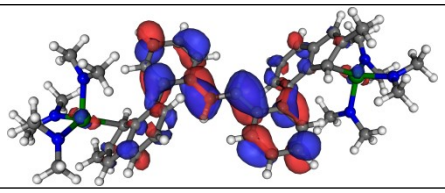

LUMO

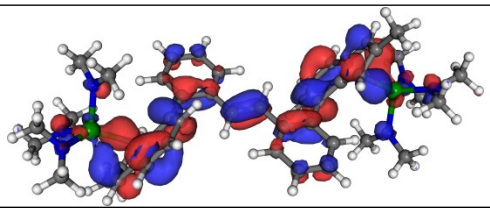

HOMO-2

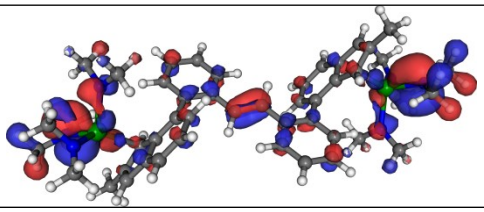

HOMO-4

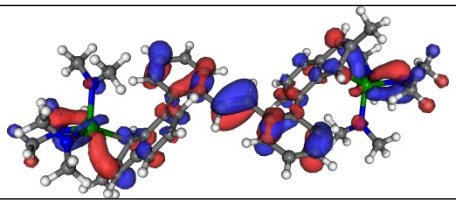

HOMO-8

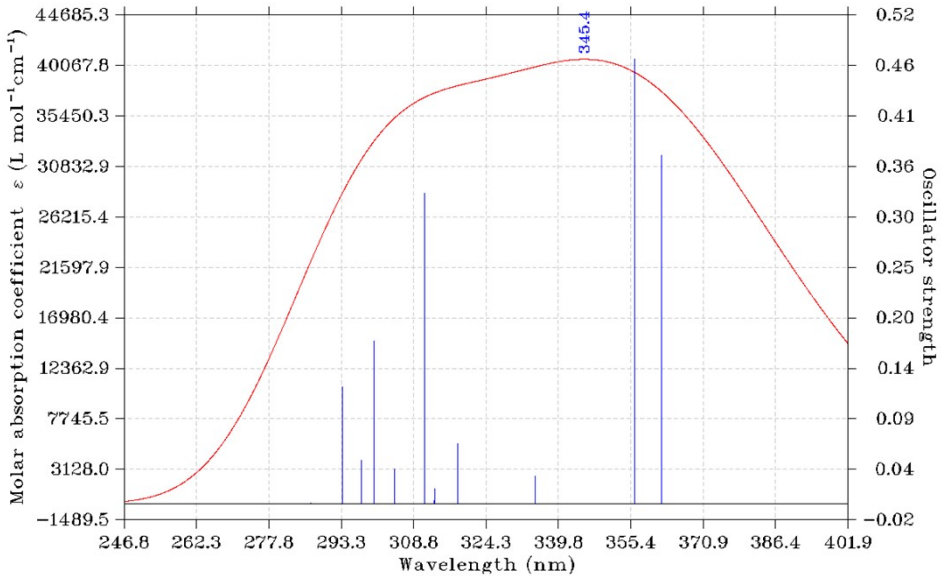

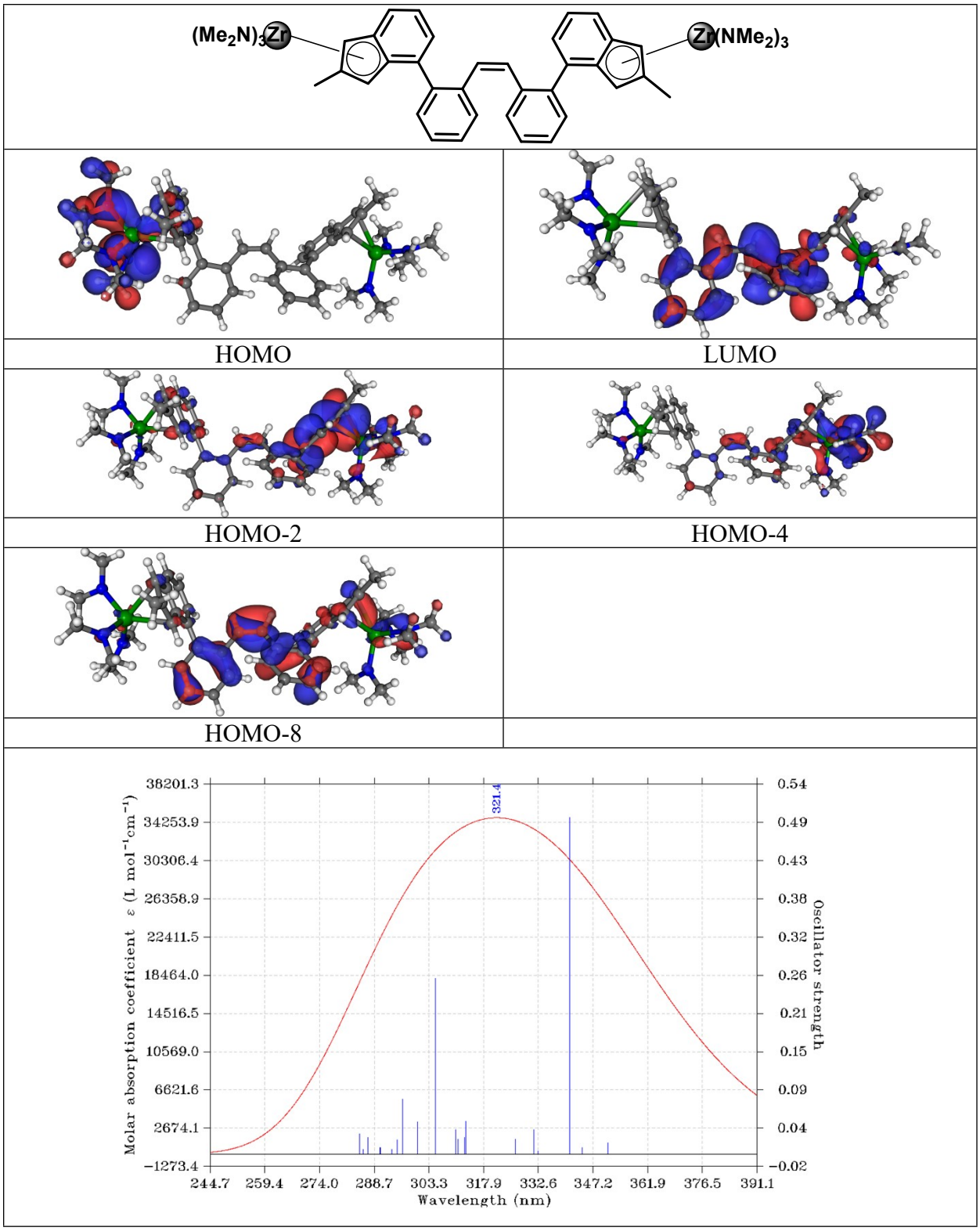

Figure S38. Relevant Kohn-Sham orbitals and absorption spectra calculated for {*o*-(*E*/*Z*)-{BisIndSB}($Zr(NMe_2)_3$)$_2$ complexes.

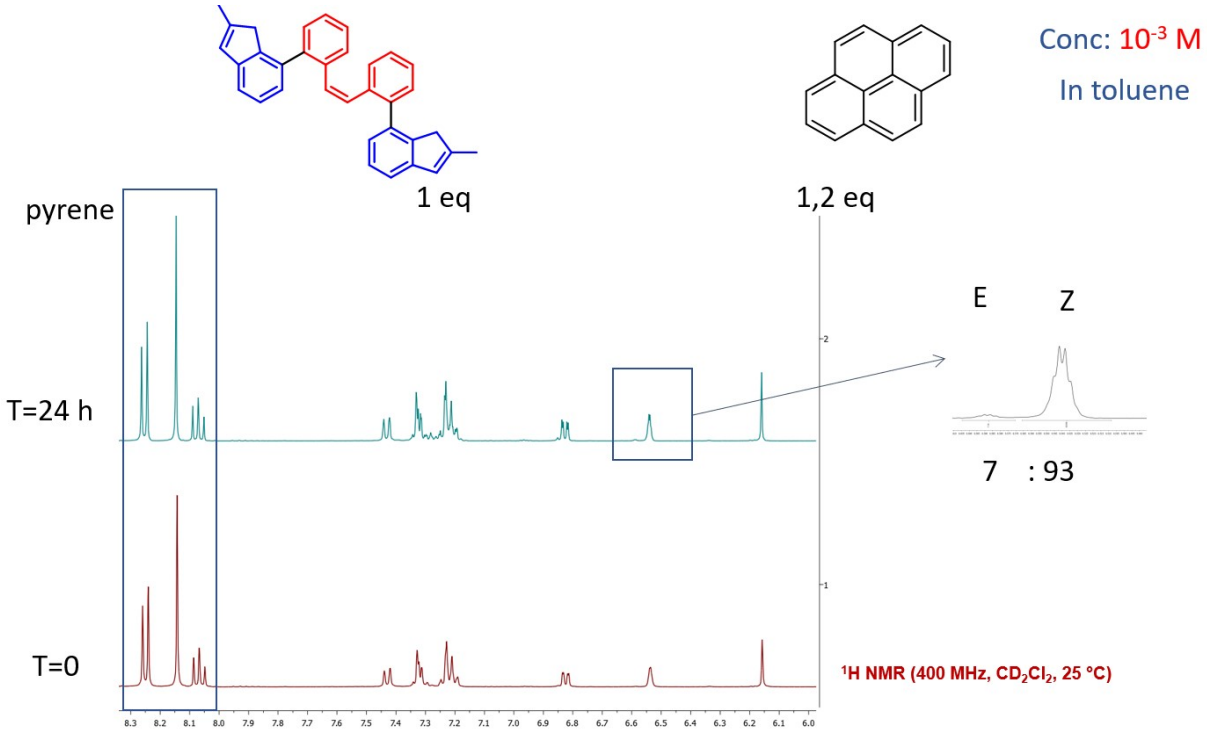

Figure S39. Photosensitized stilbene isomerization (330 nm) of {*o*-(*Z*)-BisIndSB}H_2 proligand by pyrene monitored by ^{1}H NMR (400 MHz, CD_2Cl_2, 23 °C).

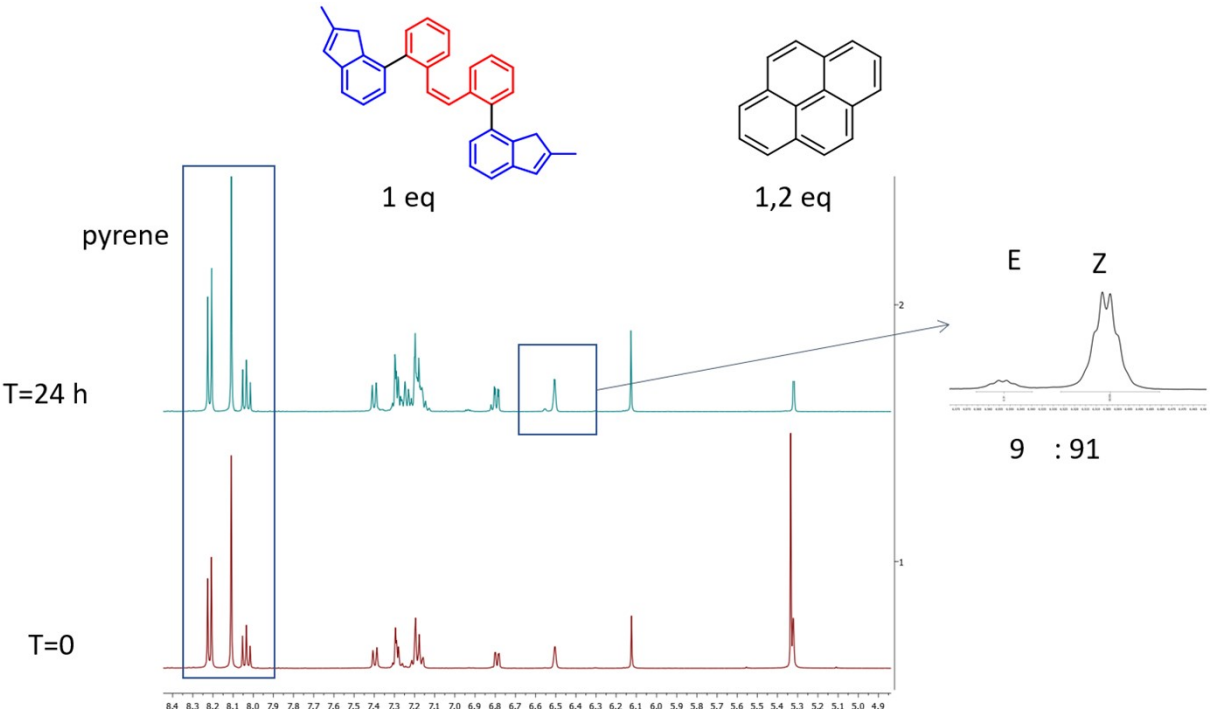

Figure S40. Photosensitized stilbene isomerization (350 nm) of {*o*-(*Z*)-BisIndSB}H_2 proligand by pyrene monitored by ^{1}H NMR (400 MHz, CD_2Cl_2, 23 °C).

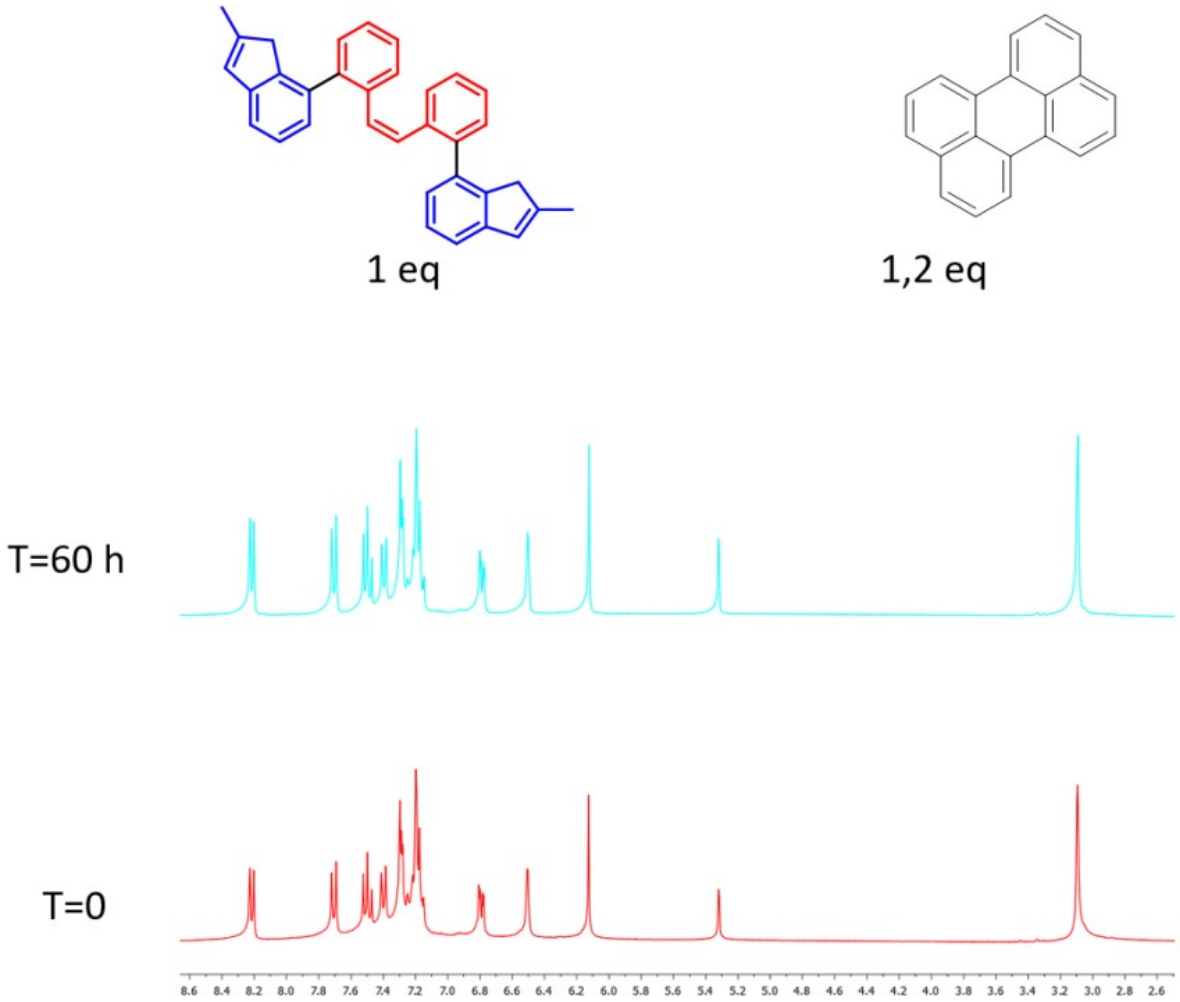

Figure S41. Attempted photosensitized stilbene isomerization (450 nm) of {*o*-(*Z*)-BisIndSB}H_2 proligand by perylene monitored by ^{1}H NMR (400 MHz, CD_2Cl_2, 25 °C).

Table S1. Summary of Crystal and Refinement Data for Compounds.

	***o*-(*E*)-SBBr$_2$**	***o*-(*Z*)-SBBr$_2$**	***m*-(*E*)-SBBr$_2$**	***o*-(*E*)-(BisIndSB)H$_2$**	***o*-(Z)-(BisIndSB)H$_2$**
CCDC number	2322681	2322682	2322680	1894661	1894662
Empirical formula	C14H10Br2	C14H10Br2	C14H10Br2	C34H28	C34H28
Formula weight	338.04	338.04	338.04	436.56	436.56
Temperature, K	295(2)	150(2)	150(2)	150(2)	150(2)
Wavelength, Å	0.71073	0.71073	0.71073	0.71073	0.71073
Crystal system	orthorombic	Monoclinic	Monoclinic	Monoclinic	Triclinic
Space group	P 2n 2ab	P 21/c	P 21/c	P 21/c	P -1
a, Å	13.8322(7)	15.6067(17)	9.7654(17)	12.0376(7)	9.4590(8)
b, Å	11.7938(6)	14.7909(18)	3.9608(7)	7.4582(4)	9.7392(7)
c, Å	15.1516(7)	11.1941(15)	15.486(2)	14.0803(6)	13.9219(11)
α	90	90	90	90	107.331(2)
β	90	108.258(5)	93.132(6)	90.605(2)	100.800(3)
γ	90	90	90	90	91.401(2)
Volume, Å^3	2471.7(2)	2453.9(5)	598.09(17)	1264.04(11)	1198.20(16)
Z	8	8	2	2	2
Density (calc.), Mg/m^3	1.817	1.830	1.877	1.147	1.210
Absorption coefficient,mm^{-1}	6.527	6.575	6.744	0.065	0.068
Crystal size, mm^3	0.36 × 0.22 × 0.15	0.560 × 0.470 × 0.310	0.600 × 0.500 × 0.200	0.310 × 0.190 ×0.150	0.290 × 0.260 × 0.120
Reflections collected	11215	23636	5387	10764	27906
Independent reflections	2831 [R(int) = 0.0415]	5628 [R(int) = 0.0578]	1357 [R(int) = 0.0554]	2885 [R(int) = 0.0505]	5479 [R(int) = 0.0720]
Max. and min. transmission	0.376 and 0.245	0.130 and 0.060	0.260 and 0.076	0.990 and 0.839	0.992 and 0.873
Data / restraints / parameters	2831 / 0 / 145	5608 / 0 / 289	1357 / 0 / 74	2885 / 0 / 155	5479 / 0 / 309
Final R indices [I>2σ(I)]	R1 = 0.0455	R1 = 0.0343	R1 = 0.0519	R1 = 0.0490	R1 = 0.0474
	wR2 = 0.0882	wR2 = 0.0744	wR2 = 0.1403	wR2 = 0.1291	wR2 = 0.1159
R indices (all data)	R1 = 0.1003	R1 = 0.0504	R1 = 0.0572	R1 = 0.0595	R1 = 0.0627
	wR2 = 0.1036	wR2 = 0.0809	wR2 = 0.1454	wR2 = 0.1357	wR2 = 0.1269
Goodness-of-fit on F^2	1.027	1.018	1.076	1.062	1.035
Largest diff. peak, e.Å^{-3}	0.460 and –0.756	1.064 and –1.117	1.537 and –1.616	0.202 and –0.178	0.258 and –0.238

Table S1 (continued)

	***o*-(*Z*)-(BisIndSB}($ZrCl_2Cp^*$)$_2$**	***m*-(*E*)-(BisIndSB}($ZrCl_2Cp^*$)$_2$**	***o*-(*E*)-(BisIndSB)($Zr(NMe_2)_3$)$_2$**
CCDC number	2322683	2322679	1894663
Empirical formula	C54 H56 Cl4 Zr2	C54 H56 Cl4 Zr2, 3 (C7 H8)	C46 H62 N6 Zr2
Formula weight	1029.22	1305.63	881.45
Temperature, K	150(2)	150(2)	150(2)
Wavelength, Å	0.71073	0.71073	0.71073
Crystal system	Monoclinic	Triclinic	Triclinic
Space group	P 21/n	P -1	P -1
a, Å	9.0237(12)	15.2349(11)	8.0140(7)
b, Å	13.1611(14)	16.0237(11)	9.0810(9)
c, Å	39.397(4)	16.3054(12)	17.2090(16)
α	90	118.098(2)	80.724(3)
β	92.514(3)	103.060(3)	78.474(3)
γ	90	90.216(2)	64.123(3)
Volume, $Å^3$	4674.4(9)	3392.3(4)	1100.20(18)
Z	4	2	1
Density (calc.), Mg/m^3	1.463	1.278	1.330
Absorption coefficient,mm^{-1}	0.711	0.505	0.511
Crystal size, mm^3	0.200 × 0.180 × 0.080	0.330 × 0.240 × 0.110	0.600 × 0.350 × 0.27
Reflections collected	25061	73188	26221
Independent reflections	10383 [R(int) = 0.0525]	15544 [R(int) = 0.0450]	5042 [R(int) = 0.0271]
Max. and min. transmission	0.945 and 0.788	0.916 and 0.862	0.871 and 0.801
Data / restraints / parameters	10383 / 0 / 392	15544 / 0 / 601	5042 / 0 / 251
Final R indices [I>2σ(I)]	R1 = 0.1115	R1 = 0.0536	R1 = 0.0220
	wR2 = 0.2931	wR2 = 0.1394	wR2 = 0.0556
R indices (all data)	R1 = 0.1172	R1 = 0.0663	R1 = 0.0240
	wR2 = 0.2972	wR2 = 0.1470	wR2 = 0.0565
Goodness-of-fit on F^2	1.111	1.036	1.119
Largest diff. peak, $e.Å^{-3}$	2.208 and –2.706	1.364 and –1.741	0.413 and –0.446

Preparation of mononuclear reference complexes for olefin polymerization

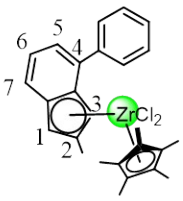

(η^5-2-Methyl-4-phenyl-indenyl)(η^5-pentamethylcyclopentadienyl)$ZrCl_2$ (**mono-1**).[1] A solution of PhMgBr (0.498 mL of a 2.4 M solution in THF, 1.19 mmol**)** was added onto $ZnCl_2$ (0.190 g, 1.39 mmol) in THF (12 mL). The cloudy solution was stirred for 1 h. Volatiles were removed under vacuum to obtain a white sticky solid. A solution of (η^5-2-methyl-4-bromo-indenyl)(η^5-pentamethylcyclopentadienyl)$ZrCl_2$ (0.500 g, 1.0 mmol), Pd(P*t*Bu)$_3$ (0.013 g, 0.025 mmol) in THF (20 mL) was added onto the white solid. The reaction mixture was stirred for 4 h, the color changing from yellow to orange. THF was removed as much as possible under vacuum. The orange oil obtained was solubilized in toluene (10 mL) and filtered over celite. Addition of a few drops of pentane resulted in the precipitation of a black solid that was filtered off. The solution was evaporated and the solid residue was recrystallized to give **mono-1** as a yellow crystalline solid (0.450 g, 91%). ^{1}H NMR (400 MHz, CD_2Cl_2, 25 °C) (Figure S42): δ 7.72–7.67 (m, 2H, 2,6-H Ph), 7.50–7.44-7.28 (m, 4H, 7-H indenyl and 3,4,5-H Ph), 7.24 (d, *J* = 7.5 Hz, 1H, 5-H indenyl), 7.08 (s, 1H, 6-H indenyl), 6.74 (dd, *J* = 2.0, 1.1 Hz, 1H, 1-H indenyl), 6.25 (d, *J* = 2.3 Hz, 1H, 3-H indenyl), 2.20 (s, 3H, 2-Me indenyl), 2.02 (s, 15H, C_5Me_5).

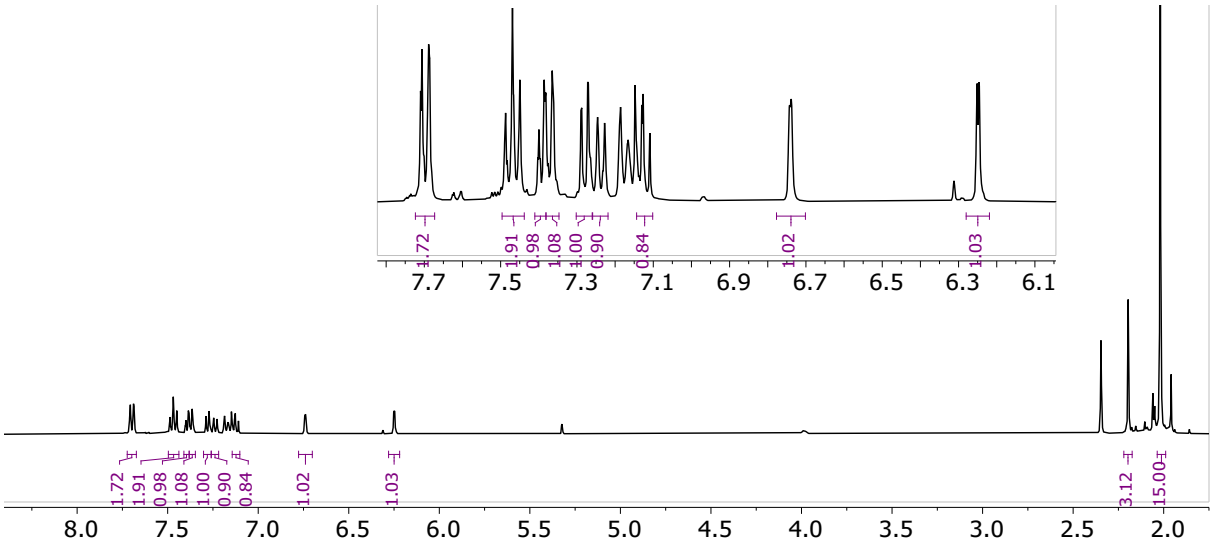

Figure S42. ^{1}H NMR (400 MHz, CD_2Cl_2, 25 °C) spectrum of (η^5-2-methyl-4-phenyl-indenyl)(η^5-pentamethylcyclopentadienyl)$ZrCl_2$ (**mono-1**).

[1] Ryabov, A. N.; Izmer, V. V.; Tzarev, A. A.; Uborsky, D. V.; Asachenko, A. F.; Nikulin, M. V.; Canich, J. A. M.; Voskoboynikov, A. Z. *Organometallics* **2009**, *28*, 3614–3617.

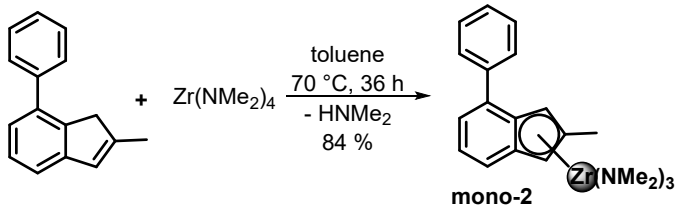

(η^5-2-Methyl-4-phenyl-indenyl)Zr(NMe$_2$)$_3$ (mono-2). In a Schlenk flask containing 2-methyl-7-phenyl-1*H*-indene (0.112 g, 0.54 mmol, 1.0 equiv) and Zr(NMe$_2$)$_4$ (0.146 g, 0.69 mmol, 2.0 equiv), toluene (10 mL) was added. The resulting solution was heated at 70 ° C for 36 h and, over this time period, volatiles were stripped every 3 h. The reaction mixture was cooled to room temperature and volatiles were removed under vacuum. The crude mixture was washed with hexanes (3 × 5 mL) and dried under vacuum, to give **mono-2** as a yellow glassy solid (0.195 g, 84%). ^{1}H NMR (400 MHz, C_6D_6, 25 °C): δ 7.74 (dd, *J* = 8.2, 1.2, 2H), 7.46 (d, *J* = 7.8, 1H), 7.35 (t, *J* = 7.6, 2H), 7.21 (t, *J* = 7.4, 1H), 7.05–6.96 (m, 2H), 6.31 (d, *J* = 2.2, 1H), 6.14 (d, *J* = 2.3, 1H), 2.75 (s, 18H, NMe$_2$)), 2.14 (s, 3H, Me indenyl). ^{13}C{^{1}H} NMR (100 MHz, C_6D_6, 25 °C): δ 141.1 (Cquat), 135.7 (Cquat), 132.0 (Cquat), 128.50, 128.36, 127.06, 124.6 (Cquat), 123.0, 122.5, 121.1, 99.6 (CH Ind), 98.2 (CH Ind), 43.9 (NMe$_2$), 14.4 (CH$_3$ Ind). iASAP-MS: *m/z* calcd for $C_{22}H_{32}N_3Zr$ [M+H]$^+$: 428.1643; found: 428.1643.

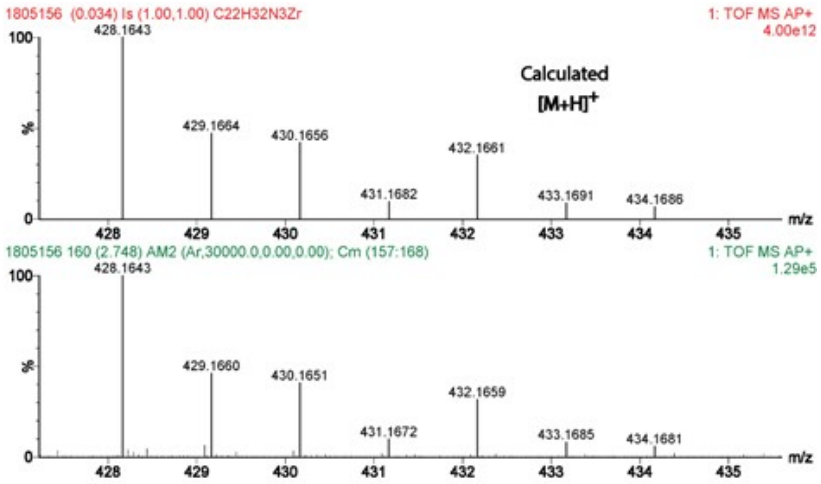

Figure S43. PiASAP MSMS spectrum of **mono-2**. The applied sampling cone and collision energy used were 10V and 5 eV, respectively.

Table S2. Ethylene polymerization experiments performed with dinuclear complexes {*m/p*-(*E/Z*)-BisIndSB}($ZrCl_2Cp^*)_2$ and the mononuclear reference complex (η^5-2-methyl-4-phenyl-indenyl)(η^5-pentamethylcyclopentadienyl)$ZrCl_2$ (**mono-1**).[a]

Entry	Comp.[a]	Temp max (°C)[b]	m(PE) (g)[c]	Prod. (kg.mol^{-1}.h^{-1})[d]	T_m (°C)[e]	ΔH_m (J g^{-1})[e]	T_{cryst} (°C)[e]	M_n (g mol^{-1})[f]	M_w (g mol^{-1})[f]	D_M[f]
NR2082	mono-**1**	60	3.89	3894	132	179	115	59,000	242,100	4.1
NR2080	*m*-(*E*)	62	4.53	4529	132	170	116	65,000	236,000	3.6
NR2146	*m*-(Z)[g]	58	4.20	4198	132	159	118	73,500	287,300	3.9
NR2143	*m*-(Z)[g]	59	3.98	3983	130	119	118	93,000	377,100	4.1
NR2137	*p*-(*E*)	61	3.67	3670	133	176	118	57,100	221,200	3.9
NR2128	*p*-(Z)	62	5.03	5027	132	161	118	64,600	247,700	3.8
NR2130	*p*-(Z)	61	5.23	5232	130	131	118	71,300	276,500	3.9

[a] Polymerization conducted in a 300-mL glass reactor equipped with a Pelton turbine, in 150 mL of toluene, with [Zr] = 1.0 µmol, 1000 equiv of MAO vs. Zr, at 50 °C initial temperature, 4 barg ethylene constant pressure; reactions were quenched after 30 min. [b] Maximal temperature recorded in the polymerization reactor. [c] Amount of polymer collected. [d] Catalytic productivity in kg(polymer) mol(Zr)$^{-1}$ h^{-1}). [e] Melting (T_m) temperature, melting enthalpy (ΔH_m) and crystallization temperature (T_{cryst}) as determined by DSC performed at the TotalEnergies research center at a heating rate of 10 °C min^{-1}; first and second runs were recorded after cooling to 30 °C; the reported melting temperatures correspond to the second run and the crystallization temperatures to the first run. [f] Number-average (M_n), weight-average (M_w) molecular weights and dispersity (D_M) as determined by SEC at 135 °C in 1,2,4-trichlorobenzene at the TotalEnergies research center in Feluy (Belgium), using polystyrene standards for universal calibration. [g] Experiments conducted with a ca. 1:1 mixture of (*E*)- and (*Z*)- isomers.

Table S3. 1-Hexene polymerization experiments performed with dinuclear complexes {*m/p*-(*E/Z*)-BisIndSB}($ZrCl_2Cp^*)_2$ and the mononuclear reference complex (η^5-2-methyl-4-phenyl-indenyl)(η^5-pentamethylcyclopentadienyl)$ZrCl_2$ (**mono-1**).[a]

Entry	Comp.[a]	m(PH) (g)[b]	Yield (%)[c]	Prod. (kg.mol^{-1}.h^{-1})[d]	M_n (g mol^{-1})[e]	D_M[e]
NR2066	mono-**1**	1.12	17	2240	8,000	2.2
NR2085	mono-**1**	0.93	14	1860	11,200	2.3
NR2067	*m*-(*E*)	0.45	7	900	7,500	2.0
NR2086	*m*-(*E*)	0.47	7	940	8,100	2.2
NR2144	*m*-(Z)[f]	0.17	3	340	19,000	2.2
NR2145	*m*-(Z)[f]	0.12	2	240	19,000	2.2
NR2138	*p*-(*E*)	0.22	3	440	12,900	2.0
NR2139	*p*-(*E*)	0.26	4	520	11,300	2.0
NR2135	*p*-(Z)	0.27	4	540	10,800	1.9
NR2136	*p*-(Z)	0.23	3	460	10,100	1.9

[a] Polymerization conducted in a glass Schlenk flask equipped with a magnetic stir bar, in 50 mL of toluene, with [Zr] = 1.0 µmol, 1000 equiv of MAO vs. Zr, 10 mL of 1-hexene, at 50 °C initial temperature; reactions were quenched after 30 min. [b] Amount of polymer collected. [c] Yield of polymer recovered. [d-e] See Table S2. [f] Experiments conducted with a ca. 1:1 mixture of (*E*)- and (*Z*)- isomers.

Table S4. Ethylene/1-hexene copolymerization experiments performed with dinuclear complexes {*m/p*-(*E/Z*)-BisIndSB}($ZrCl_2Cp^*$)$_2$ and the mononuclear reference complex (η^5-2-methyl-4-phenyl-indenyl)(η^5-pentamethylcyclopentadienyl)$ZrCl_2$ (**mono-1**).[a]

Entry	Comp.[a]	Temp max (°C)[b]	m(pol) (g)[c]	Prod. (kg.mol^{-1}.h^{-1})[d]	T_m (°C)[e]	ΔH_m (J g^{-1})[e]	T_{cryst} (°C)[e]	M_n (g mol^{-1})[f]	M_w (g mol^{-1})[f]	D_M[f]	1-hex (wt%)[h]
NR2074	mono-**1**	57	4.40	4400	118	119	105	47,700	218,900	4.6	4.1
NR2077	*m*-(*E*)	59	5.64	5641	118	128	104	39,100	164,900	4.2	4.7
NR2087	*m*-(*E*)	64	6.68	6681	118	129	103	36,900	151,900	4.1	4.9
NR2149	*m*-(Z)[g]	60	3.22	3221	118	108	107	48,700	212,400	4.4	4.3
NR2150	*m*-(Z)[g]	62	4.50	4502	119	108	107	39,000	185,500	4.8	4.3
NR2141	*p*-(*E*)	65	5.79	5786	120	117	107	40,600	187,500	4.6	4.0
NR2142	*p*-(*E*)	65	6.28	6281	119	113	107	39,400	181,600	4.6	4.0
NR2132	*p*-(Z)	65	6.39	6393	120	116	107	40,000	186,700	4.7	4.0
NR2133	*p*-(Z)	65	6.18	6184	120	122	107	40,200	192,900	4.8	4.0

[a] Polymerization conducted in a 300-mL glass reactor equipped with a Pelton turbine, in 100 mL of toluene, with [Zr] = 1.0 µmol, 1000 equiv of MAO vs. Zr, at 50 °C initial temperature, 4 barg ethylene constant pressure and 2.5 mL (0.02 mol) of 1-hexene; reactions were quenched after 30 min. [b-g] See Table S2. [h] Amount of 1-hexene incorporated in the copolymer, as determined by ^{13}C NMR spectroscopy.

Table S5. Ethylene polymerization experiments performed with dinuclear complexes {*o*-(*E/Z*)-BisIndSB}($Zr(NMe_2)_3$)$_2$ and the mononuclear reference complex (η^5-2-methyl-4-phenyl-indenyl)$Zr(NMe_2)_3$ (**mono-2**).[a,f]

Entry	Comp.[a]	m(PE) (g)[b]	Prod. (kg.mol^{-1}.h^{-1})[c]	T_m (°C)[d]	T_{cryst} (°C)[d]
TC1	mono-**2**	0.358	955	135	119
TC2	mono-**2**	0.420	1120	135	119
TC3	*o*-(*E*)-Bis(Ind)	0.293	781	134	119
TC4	*o*-(*E*)-Bis(Ind)	0.310	827	134	119
TC5	*o*-(*Z*)-Bis(Ind)	0.256	683	135	118
TC6	*o*-(*Z*)-Bis(Ind)	0.223	595	135	118

[a] Polymerization conducted in a 300-mL glass reactor equipped with a Pelton turbine, in 150 mL of toluene, with [Zr] = 1.0 µmol, 5000 equiv of MAO vs. Zr, at 50 °C initial temperature, 4 barg ethylene constant pressure; reactions were quenched after 15 min. [b] Amount of polymer collected. [c] Catalytic productivity in kg(polymer) mol(Zr)$^{-1}$ h^{-1}). [d] Melting (T_m) and crystallization (T_{cryst}) temperatures as determined by DSC performed at a heating rate of 10 °C min^{-1}; first and second runs were recorded after cooling to 30 °C; the reported melting temperatures correspond to the second run and the crystallization temperatures to the first run. [f] Note that none of the polymers were soluble at 135 °C in 1,2,4-trichlorobenzene, hence no SEC measurements could be conducted.

Table S6. Ethylene/1-hexene copolymerization experiments performed with dinuclear complexes {*o*-(*E/Z*)-BisIndSB}($Zr(NMe_2)_3)_2$ and the mononuclear reference complex (η^5-2-methyl-4-phenyl-indenyl)$Zr(NMe_2)_3$ (**mono-2**).[a]

Entry	Comp. [a]	m(pol) (g) [b]	Prod. ($kg.mol^{-1}.h^{-1}$) [c]	T_m (°C) [d]	T_{cryst} (°C) [d]
TC1	mono-**2**	0.311	415	122	111
TC2	mono-**2**	0.295	393	122	112
TC3	*o*-(*E*)-Bis(Ind)	0.320	427	125	113
TC4	*o*-(*E*)-Bis(Ind)	0.275	367	125	113
TC5	*o*-(*Z*)-Bis(Ind)	0.258	344	125	113
TC6	*o*-(*Z*)-Bis(Ind)	0.279	372	125	113

[a] Polymerization conducted in a 300-mL glass reactor equipped with a Pelton turbine, in 150 mL of toluene, with [Zr] = 1.0 µmol, 5000 equiv of MAO vs. Zr, at 50 °C initial temperature, 4 barg ethylene constant pressure, 2.5 mL (0.02 mol) of 1-hexene; reactions were quenched after 30 min. [b] Amount of polymer collected. [c] Catalytic productivity in kg(polymer) $mol(Zr)^{-1}$ h^{-1}). [d] Melting (T_m) and crystallization (T_{cryst}) temperatures as determined by DSC performed at a heating rate of 10 °C min^{-1}; first and second runs were recorded after cooling to 30 °C; the reported melting temperatures correspond to the second run and the crystallization temperatures to the first run.

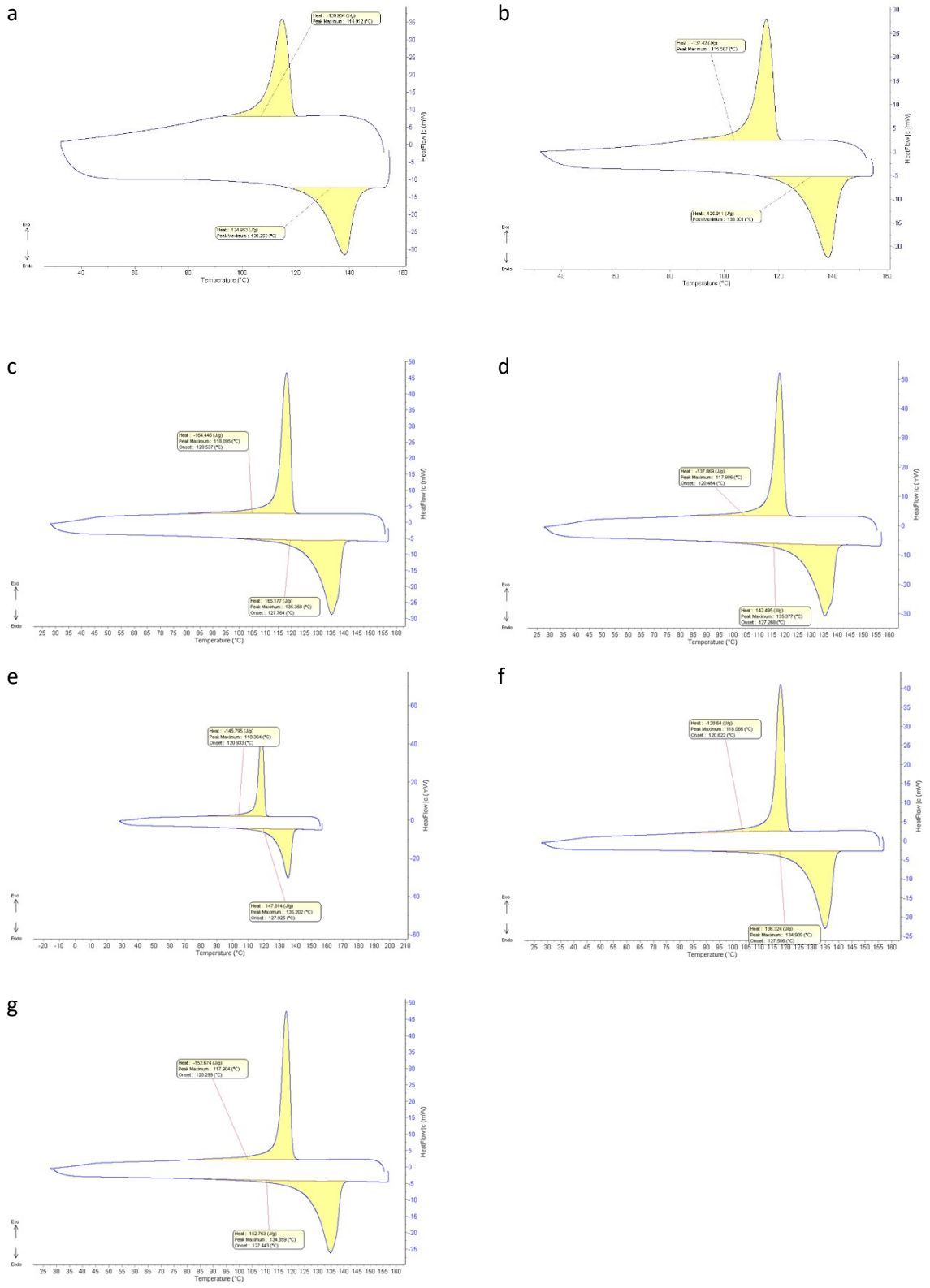

Figure S44. Representative DSC traces of polyethylene samples corresponding to a) NR2082, b) NR2080, c) NR2146, d) NR2143, e) NR2137, f) NR2128, g) NR2130 entries from Table S2.

a

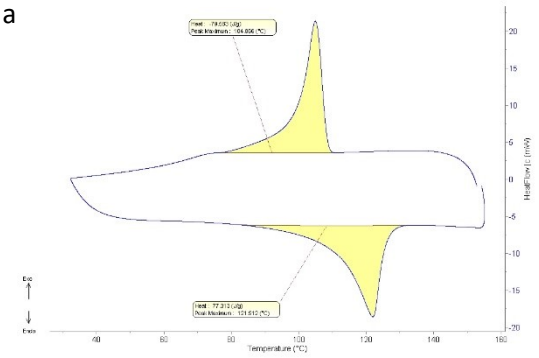
Exo
Endo
Temperature (°C)
HeatFlow (c (mW)

b

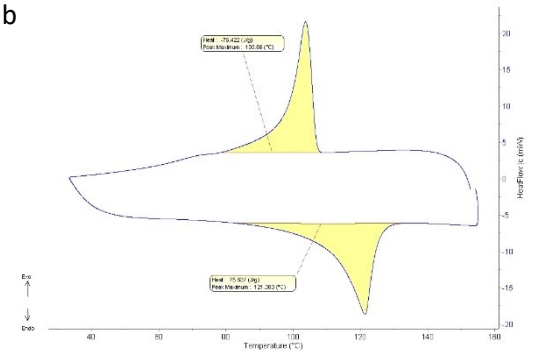
Exo
Endo
Temperature (°C)
HeatFlow (c (mW)

c

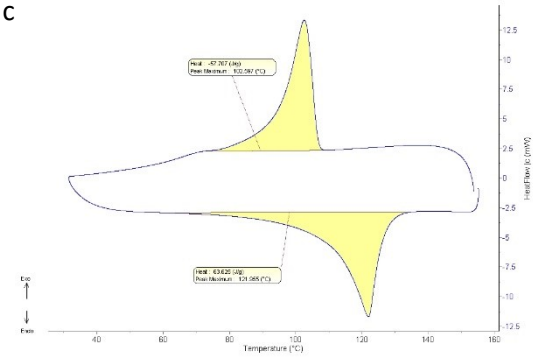
Exo
Endo
Temperature (°C)
HeatFlow (c (mW)

d

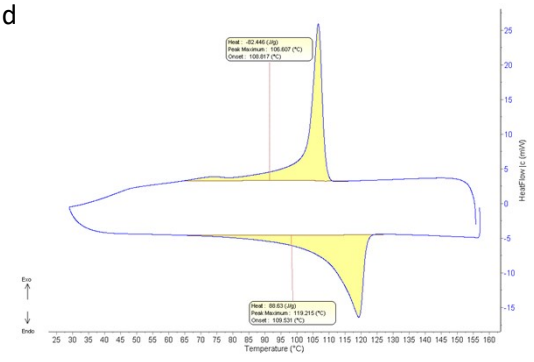
Exo
Endo
Temperature (°C)
HeatFlow (c (mW)

e

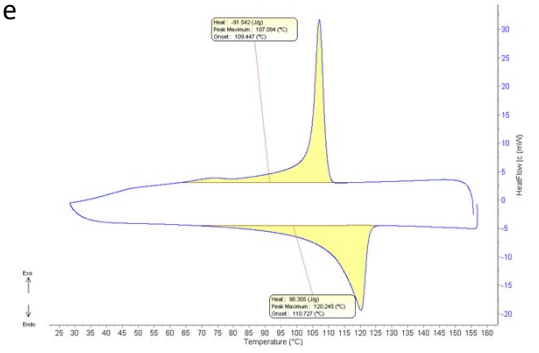
Exo
Endo
Temperature (°C)
HeatFlow (c (mW)

f

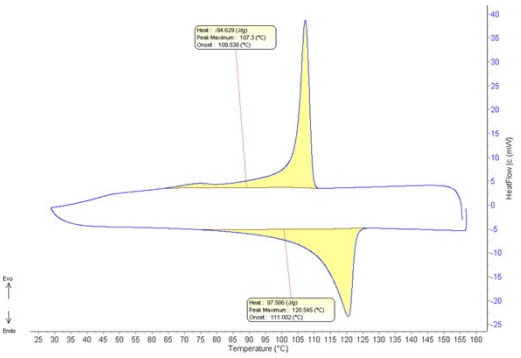
Exo
Endo
Temperature (°C)
HeatFlow (c (mW)

g

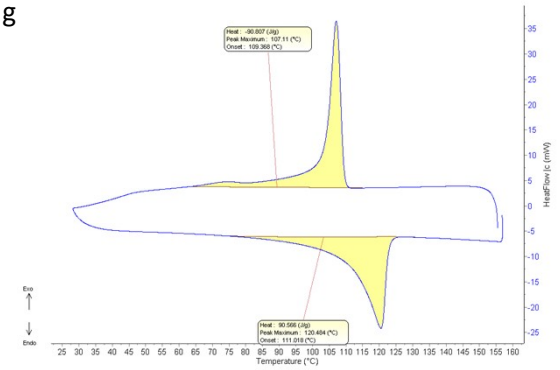
Exo
Endo
Temperature (°C)
HeatFlow (c (mW)

h

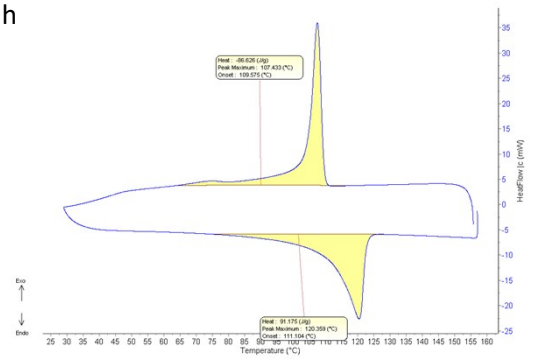
Exo
Endo
Temperature (°C)
HeatFlow (c (mW)

i

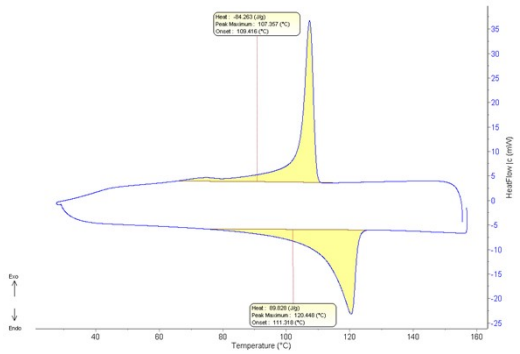

Figure S45. Representative DSC traces of ethylene / 1-hexene copolymer samples corresponding to a) NR2074, b) NR2077, c) NR2087, d) NR2149, e) NR2150, f) NR2141, g) NR2142, h) NR2132 and i) entries from Table S4.

a

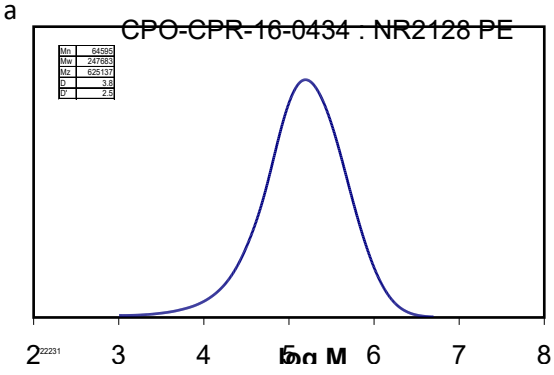
CPO-CPR-16-0434 . NR2128 PE
Mn 64595
Mw 247683
Mz 625137
D 3.8
D' 2.5
2 3 4 6 7 8

b

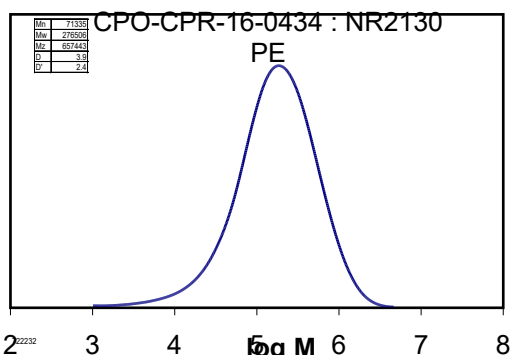
CPO-CPR-16-0434 : NR2130 PE
Mn 71335
Mw 276506
Mz 657443
D 3.9
D' 2.4
2 3 4 6 7 8

c

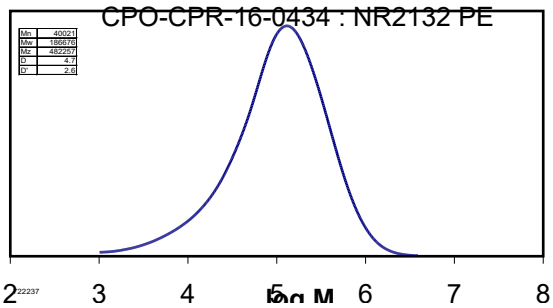
CPO-CPR-16-0434 : NR2132 PE
Mn 40021
Mw 186676
Mz 482257
D 4.7
D' 2.6
2 3 4 6 7 8

d

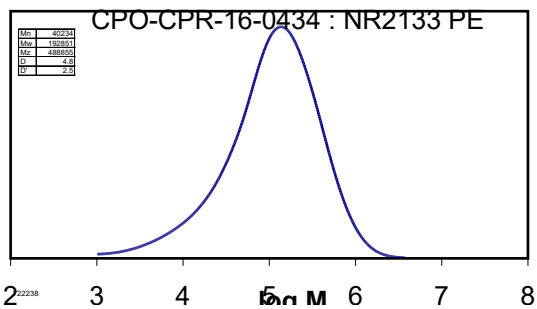
CPO-CPR-16-0434 : NR2133 PE
Mn 40234
Mw 192851
Mz 488856
D 4.8
D' 2.5
2 3 4 6 7 8

e

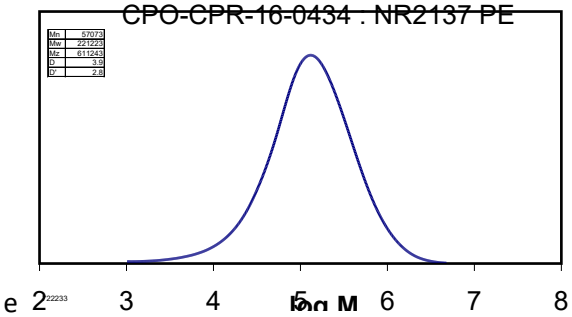
CPO-CPR-16-0434 . NR2137 PE
Mn 57073
Mw 221233
Mz 611243
D 3.9
D' 2.8
2 3 4 6 7 8

f

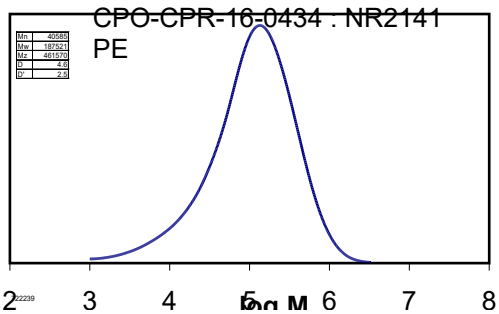
CPO-CPR-16-0434 : NR2141 PE
Mn 40589
Mw 187521
Mz 461570
D 4.6
D' 2.5
2 3 4 6 7 8

g

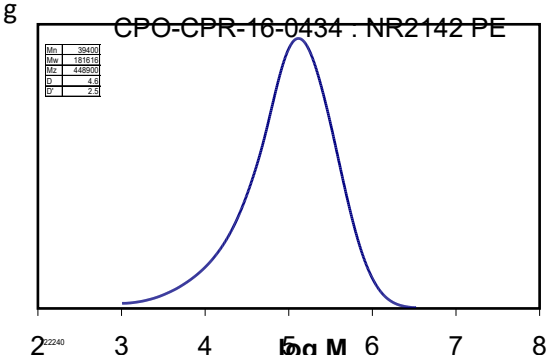
CPO-CPR-16-0434 . NR2142 PE
Mn 39400
Mw 181616
Mz 448900
D 4.6
D' 2.5
2 3 4 6 7 8

h

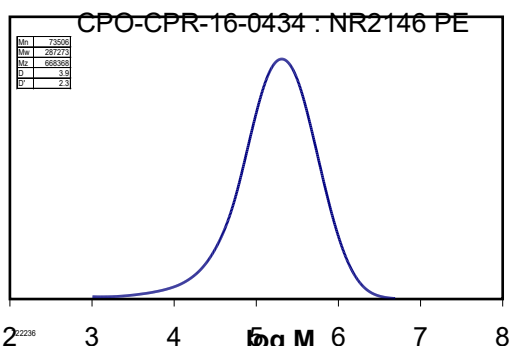
CPO-CPR-16-0434 : NR2146 PE
Mn 73506
Mw 287273
Mz 668368
D 3.9
D' 2.3
2 3 4 6 7 8

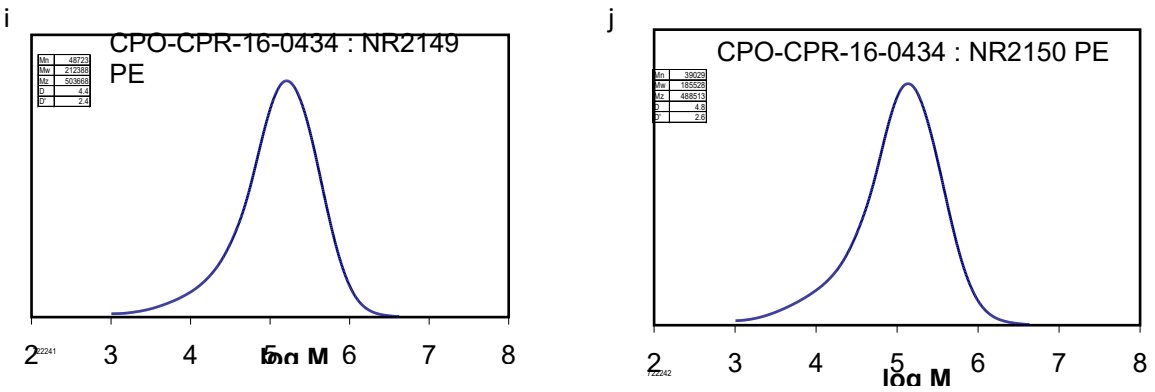

Figure S46. Representative Size Exclusion Chromatography traces of polyethylene and ethylene / 1-hexene copolymer samples of: a) Entry NR2108 from Table S2, b) Entry NR2130 from Table S2, c) Entry NR2132 from Table S4, d) Entry NR2133 from Table S4, e) Entry NR2137 from Table S2, f) Entry NR2141 from Table S4, g) Entry NR2142 from Table S4, h) Entry NR2146 from Table S2, i) Entry NR2149 from Table S4, j) Entry NR2150 from Table S4,